

AD-A104 675

SCHOOL OF AEROSPACE MEDICINE BROOKS AFB TX  
OPTOACOUSTIC SPECTROSCOPY TO DETECT HYDRAZINE FUELS. (U)  
JUL 81 E S KOLESAR

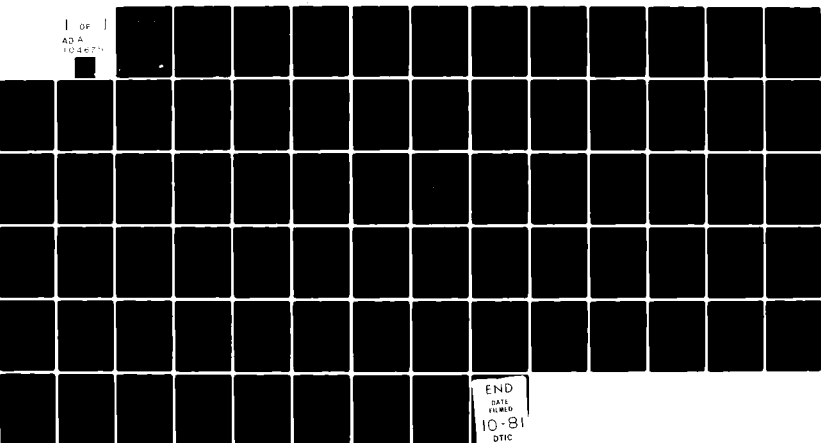
F/G 14/2

UNCLASSIFIED

SAM-TR-81-15

NL

1 OF 1  
ADA  
A104675



END  
DATE  
FILED  
10-81  
DTIC

AD A104675

Report SAM-TR-81-15

12

## OPTOACOUSTIC SPECTROSCOPY TO DETECT HYDRAZINE FUELS

Edward S. Kolesar, Jr., Captain, USAF

DTIC  
FOLIO 1  
SEP 29 1981

July 1981

Final Report for Period 1 May 1979 - 1 February 1980

Approved for public release; distribution unlimited.

USAF SCHOOL OF AEROSPACE MEDICINE  
Aerospace Medical Division (AFSC)  
Brooks Air Force Base, Texas 78235



## NOTICES

This final report was submitted by personnel of the Crew Environments Branch, Crew Technology Division, USAF School of Aerospace Medicine, Aerospace Medical Division, AFSC, Brooks Air Force Base, Texas, under job order 7930-11-36.

When U.S. Government drawings, specifications, or other data are used for any purpose other than a definitely related Government procurement operation, the Government thereby incurs no responsibility nor any obligation whatsoever; and the fact that the Government may have formulated, furnished, or in any way supplied the said drawings, specifications, or other data is not to be regarded by implication or otherwise, as in any manner licensing the holder or any other person or corporation, or conveying any rights or permission to manufacture, use, or sell any patented invention that may in any way be related thereto.

This report has been reviewed by the Office of Public Affairs (PA) and is releasable to the National Technical Information Service (NTIS). At NTIS, it will be available to the general public, including foreign nations.

This technical report has been reviewed and is approved for publication.

*Edward S. Kolesar, Jr.*

EDWARD S. KOLESAR, JR., Captain, USAF  
Project Scientist

*R. L. Miller*

RICHARD L. MILLER, Ph.D.  
Supervisor

*Roy L. DeHart*

ROY L. DEHART  
Colonel, USAF, MC  
Commander

UNCLASSIFIED

SECURITY CLASSIFICATION OF THIS PAGE (When Data Entered)

REPORT DOCUMENTATION PAGE

READ INSTRUCTIONS  
BEFORE COMPLETING FORM

1. REPORT NUMBER

SAM-1R-01-15

2. GOVT ACQUISITION NO.

AD-A104

3. RECOMMENDED CATALOG NUMBER

675

4. TITLE (and Subtitle)

OPTOACOUSTIC SPECTROSCOPY TO DETECT  
HYDRAZINE FUELS.

5. SECURITY CLASSIFICATION

Final Report

1 May 1979 - 1 Feb 1980

6. PERFORMING ORGANIZATION NUMBER

7. AUTHOR

Edward S. Kolesar, Jr., Captain, USAF

8. CONTRACT OR GRANT NUMBER

9. PERFORMING ORGANIZATION NAME AND ADDRESS

USAF School of Aerospace Medicine (VNL)  
Aerospace Medical Division (AFSC)  
Brooks Air Force Base, Texas 78235

10. PROGRAM ELEMENT, PROJECT, +48 AREA & WORK UNIT NUMBERS

62202F 17

7930-11-36

11. CONTROLLING OFFICE NAME AND ADDRESS

USAF School of Aerospace Medicine (VNL)  
Aerospace Medical Division (AFSC)  
Brooks Air Force Base, Texas 78235

12. REPORT DATE

July 1981

13. NUMBER OF PAGES

71

14. MONITORING AGENCY NAME & ADDRESS (if different from Controlling Office)

1/1

15. SECURITY CLASS. (of this report)

Unclassified

16. DISTRIBUTION STATEMENT (of this Report)

Approved for public release; distribution unlimited.

17. DISTRIBUTION STATEMENT (of the abstract entered in Block 20, if different from Report)

18. SUPPLEMENTARY NOTES

19. KEY WORDS (Continue on reverse side if necessary and identify by block number)

Optoacoustic	MMH	Sample cell
Optoacoustic spectroscopy	UDMH	Photoacoustic
Hydrazine	CO <sub>2</sub> laser	
	Lock-in amplifier	

20. ABSTRACT (Continue on reverse side if necessary and identify by block number)

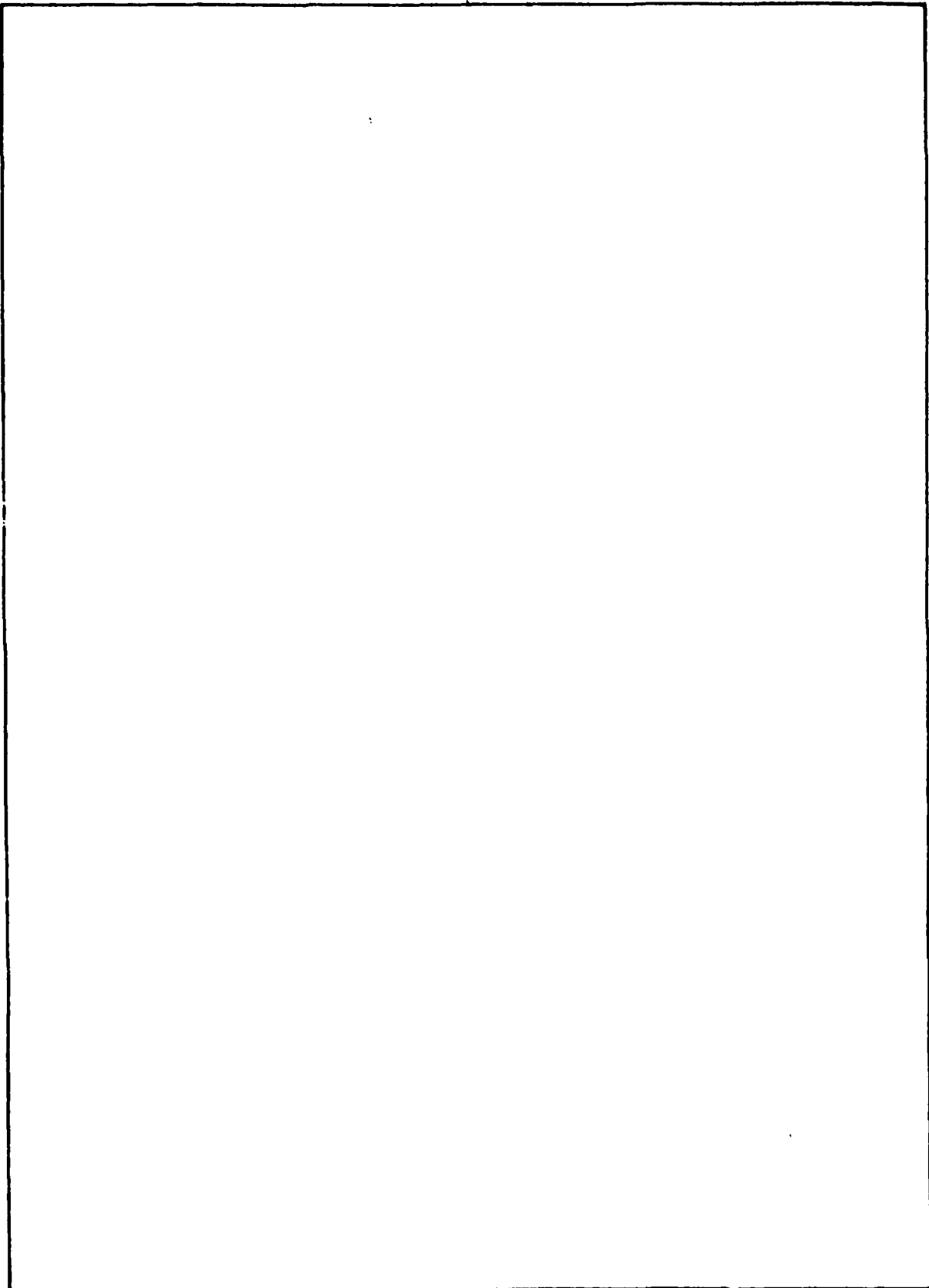
An optoacoustic spectroscopy system is analyzed with the intention of designing a specific instrument to detect the hydrazine fuels. Also presented are the criteria, cost, and theoretical principles used to accomplish the engineering design.

DD FORM 1473 EDITION OF 1 NOV 65 IS OBSOLETE  
JAN 73

UNCLASSIFIED

~~SECURITY CLASSIFICATION OF THIS PAGE (When Data Entered)~~

SECURITY CLASSIFICATION OF THIS PAGE(When Data Entered)



SECURITY CLASSIFICATION OF THIS PAGE(When Data Entered)

## CONTENTS

	<u>Page</u>
INTRODUCTION . . . . .	3
BACKGROUND . . . . .	3
GENERAL SYSTEM DESCRIPTION . . . . .	7
Acoustic Signal Generation Process . . . . .	7
Acoustic Signal Detection . . . . .	18
OPTIMUM DESIGN OF AN OPTOACOUSTIC SPECTROMETER TO DETECT HYDRAZINE FUELS .	25
Laser Wavelength Selection . . . . .	27
Variable-Speed Chopper . . . . .	34
Microphone and Preamplifier . . . . .	34
Laser Power Meter . . . . .	35
Lock-In Amplifier . . . . .	35
Ratiometer . . . . .	38
Sample Cell Design . . . . .	39
CONCLUSION . . . . .	43
REFERENCES . . . . .	48

## FIGURES

### Fig. No.

1. Optoacoustic spectrometer equipment configuration . . . . .	8
2. Condenser microphone equivalent electrical circuit . . . . .	22
3. Condenser microphone and preamplifier equivalent electrical circuit noise model . . . . .	24
4. Hydrazine absorption spectra . . . . .	28
5. Monomethylhydrazine (MMH) absorption spectra . . . . .	29
6. Absorption spectra of 1,1-dimethylhydrazine (UDMH) . . . . .	30
7. Dimensional specifications for the Sylvania model 950A laser head, laser exciter, and model 750 cooling unit . . . . .	31
8. Conventional lock-in amplifier . . . . .	38
9. Nonresonant single-pass sample cell design . . . . .	45

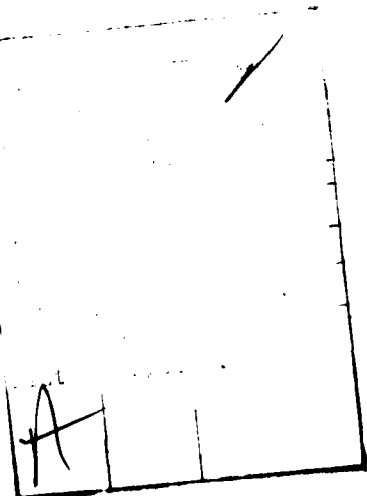
CONTENTS (Cont'd.)

<u>Fig. No.</u>		<u>Page</u>
10.	Optoacoustic spectrometer component integration for the measurement of the hydrazine fuels	46

TABLES

Table No.

1.	Laser optoacoustic spectroscopy-detectable gas sensitivities (interference-free)	4
2.	Technical characteristics of Sylvania model 950A CO <sub>2</sub> laser	32
3.	Sylvania model 950A tunable laser wavelengths (00°1 - 10°0) band	33
4.	Technical characteristics of Brue & Kjaer model 4144 air condenser microphone	36
5.	Technical characteristics of Brue & Kjaer model 2619 preamplifier and model 2804 power supply	37
6.	Technical characteristics of Coherent Radiation model 210 laser power meter	37
7.	Technical characteristics of Princeton Applied Research Corporation model 124A lock-in amplifier and model 117 preamplifier	39
8.	Technical characteristics of Princeton Applied Research model 188 precision digital ratiometer	40
9.	Summary of optimum design parameters for a hydrazine fuel optoacoustic spectrometer	44
10.	Relative optoacoustic spectrometer equipment costs	47



## OPTOACOUSTIC SPECTROSCOPY TO DETECT HYDRAZINE FUELS

### INTRODUCTION

The U.S. Air Force now has need of a portable real-time point detector, with a sensitivity of at least 0.1 ppm, for the hydrazine fuels. Therefore the purpose of this report is to present the principles and practice of optoacoustic spectroscopy and a theoretical analysis of the feasibility for using this technique to detect the gaseous hydrazine fuels (hydrazine, monomethylhydrazine {MMH}, and 1,1-dimethylhydrazine {UDMH}). The success of numerous efforts to detect small quantities of gaseous pollutants is shown in Table 1.

### BACKGROUND

The optoacoustic effect was discovered by Alexander Graham Bell over 90 years ago (30-32). In his pioneering experiments, Bell focused mechanically chopped, non-dispersed sunlight onto a sample tube. When the light fell intermittently on a solid or liquid in the sample tube and was absorbed, Bell witnessed a "sonorousness" through an attached listening tube (a short length of tubing connected to one end of the sample cell, with the other end placed in the observer's ear). The frequency of the emitted sound was that at which the incident light was modulated.

The transformation of optic to acoustic energy was reported: "...the pulses of absorbed optical quanta are degraded in the sample to heat pulses, which in a gas, express themselves as pressure pulses, that is, sound...."(32). In summarizing the sonorous effects produced in a variety of materials, Bell prophesied: "I recognize the fact that the spectrophone must ever remain a mere adjunct to the spectroscope; but I anticipate that it has a wide and independent field of usefulness in the investigation of absorption-spectra in the ultra-red" (32).

Mercadier, Preece, Roentgen, and Tyndall also reported studies of the optoacoustic effect, particularly with gases (216, 285, 298, 299, 357). Their attempts were not very successful, due to the lack of sensitive acoustic detection devices. After these early studies, no further work was reported until 1938.

In 1938, three independent investigators reported the application of the optoacoustic effect to gas analysis. Luft, Pfund, and Veingerov all described instruments for the analysis of gases and gas mixtures which utilized the optoacoustic effect to detect their absorption of infrared radiation (196, 273, 360-362).

Since then, numerous investigators have measured the vibrational relaxation rates in gases, and have presented theoretical treatments of the optoacoustic effect (4, 6, 7, 11, 12, 16, 20-27, 42, 43, 45, 47-52, 54-56, 58, 60, 61, 64, 65, 69-71, 75, 77, 80, 91, 92, 94, 95, 106, 107, 110-113, 115, 118, 119, 124, 125, 136, 148-154, 158, 160, 163, 167, 173-178, 181, 185, 188, 194, 202-205,

TABLE 1. LASER OPTOACOUSTIC SPECTROSCOPY-DETECTABLE GAS SENSITIVITIES (INTERFERENCE-FREE)

<u>Gas</u>	<u>Laser</u>	<u>Wavelength (μm)</u>	<u>Sensitivity (ppb)</u>	<u>Reference</u>
Acetonitrile	CO <sub>2</sub>	9.4 P(16)	670.0	252
Acetylene	CO <sub>2</sub>	10.4 P(14)	3.0	252
Ammonia	CO <sub>2</sub>	10.4 R(6)	5.3	252
	CO <sub>2</sub>	9.4 R(30)	0.8	252
	CO <sub>2</sub>	10.7 P(32)	1.2	204
	CO <sub>2</sub>	6.2 P(15)	0.4	176
	CO <sub>2</sub>	9.2 R(30)	0.3	318
	CO <sub>2</sub>	10.4 R(6)	1.1	318
Benzene	CO <sub>2</sub>	9.4 P(30)	48.0	252
	CO <sub>2</sub>	9.4 P(20)	143.0	252
	CO <sub>2</sub>	9.6 P(30)	3.0	176
1,3-Butadiene	CO	6.2 P(13)	1.0	175
	CO <sub>2</sub>	10.7 P(30)	2.0	176
Butane	CO <sub>2</sub>	10.4 R(14)	200.0	252
T-Butanol	CO <sub>2</sub>	10.4 P(34)	26.0	252
	CO <sub>2</sub>	10.4 P(30)	31.0	252
1-Butene	CO	6.1 P(9)	2.0	175
	CO <sub>2</sub>	10.8 P(38)	2.0	176
Cyclohexane	CO <sub>2</sub>	9.4 P(28)	250.0	252
Cyclohexanone	CO <sub>2</sub>	9.6 P(10)	20.2	71
1,2-Dichloroethane	CO <sub>2</sub>	10.4 P(10)	450.0	252
	CO <sub>2</sub>	10.4 P(22)	500.0	252
Dinitrate	CO <sub>2</sub>	9.6 P(14)	8.26	71
2,4-Dinitrotoluene	CO <sub>2</sub>	9.6 P(16)	0.5	71
Ethyl Acetate	CO <sub>2</sub>	9.4 P(6)	8.3	252
	CO <sub>2</sub>	9.4 P(14)	9.0	252
Ethylene	CO <sub>2</sub>	10.4 P(14)	2.6	252
	CO <sub>2</sub>	10.5 P(14)	0.2	176
	CO <sub>2</sub>	10.5 P(14)	0.3	177
	CO <sub>2</sub>	10.5 P(14)	0.3	330
Ethylene Glycol	CO <sub>2</sub>	9.4 P(14)	38.0	252
Freon-11	CO <sub>2</sub>	9.4 R(22)	18.0	252
Freon-12	CO <sub>2</sub>	9.4 R(20)	20.0	252
	CO <sub>2</sub>	10.4 P(30)	5.5	252
	CO <sub>2</sub>	10.8 P(42)	0.35	318
	CO <sub>2</sub>	9.2 R(32)	2.4	318

(Cont'd. on facing page)

TABLE 1. (Cont'd.)

Gas	Laser	Wavelength ( $\mu\text{m}$ )	Sensitivity (ppb)	Reference
Freon -113	$\text{CO}_2$	9.4 P(26)	5.0	252
Freon -114	$\text{CO}_2$	9.4 P(14)	3.6	252
Furan	$\text{CO}_2$	10.4 R(30)	25.0	252
Iodo Propane	$\text{CO}_2$	9.4 R(24)	360.0	252
Isopropanol	$\text{CO}_2$	10.4 P(10)	29.0	252
Methane	He-Ne	3.4	10.0	174
Methanol	$\text{CO}_2$	9.7 P(34)	0.3	176
Methyl Chloroform	$\text{CO}_2$	9.4 R(24)	11.0	252
Methyl Ethyl Ketone	$\text{CO}_2$	10.4 P(22)	83.0	252
Methylamine	$\text{CO}_2$ $\text{CO}_2$	9.4 P(24) 9.6 P(30)	120.0 25.3	252 71
Nitric Oxide	CO CO	5.2 P(11) 5.3 P(12)	0.4 10.0	176 175
Nitrogen Dioxide	CO Dye Argon	6.2 P(14) 0.5 ~ 0.6 Not reported	0.1 4.0 5.0	170 64 137
Nitroglycerine	$\text{CO}_2$ $\text{CO}_2$	9.4 P(14) 9.4 P(14)	0.7 0.23	252 71
Ozone	$\text{CO}_2$	9.4 P(14)	9.0	252
Perchloroethylene	$\text{CO}_2$ $\text{CO}_2$ $\text{CO}_2$ $\text{CO}_2$	10.4 P(42) 10.4 P(40) 10.8 P(42) 10.8 P(40)	3.2 4.3 1.1 1.4	252 252 318 318
Propylene	CO	6.1 P(9)	3.0	176
Sulfur Hexafluoride	$\text{CO}_2$	10.4 P(16)	0.2	252
Trichloroethylene	$\text{CO}_2$ $\text{CO}_2$ $\text{CO}_2$	10.4 P(20) 10.6 P(24) 10.6 P(20)	13.0 0.7 4.2	252 176 318
Vinyl Chloride	$\text{CO}_2$	10.4 P(22)	12.0	252
Water	CO	5.9 P(13)	14.0	176

207, 208, 209, 211, 212, 228, 235, 240, 246, 255, 257, 259, 262-268, 270, 271, 286, 287, 292, 294, 295, 297, 300, 303, 313-315, 318-320, 322, 330, 336, 342-345, 347, 351-356, 365-368, 370-373, 379, 381-383, 387). Refinements in the instrumentation used for optoacoustic measurements have also been reported (1, 4, 5, 9, 18, 20, 22, 24, 35-39, 41, 42, 44, 46, 54, 55, 62, 63, 66, 67, 73, 74, 78, 79, 81, 82, 84, 85, 90, 93, 96-101, 103, 104, 114, 116, 117, 120-123, 131, 132, 137, 145, 146, 149, 156, 157, 162, 168-172, 179, 180, 186, 187, 190, 193, 197, 199-202, 215, 220, 224-227, 229, 236-239, 241, 243-245, 248, 249, 252, 253, 260, 261, 269, 272, 274-276, 278, 279, 287-291, 293, 301, 302, 304, 321, 332, 334, 337, 338, 341, 348-350, 359, 364, 376, 385, 386).

In addition to studying gases by optoacoustic spectroscopy, many investigators have applied this technique to the direct examination of solid and semi-solid samples (3, 8-10, 13-15, 17, 19, 33-39, 53, 57, 12, 76, 83, 86, 114, 126-130, 133-135, 155, 159, 161, 164, 166, 182, 183, 191, 192, 195, 198, 206, 210, 213, 217, 223, 230-234, 247, 254, 258, 277, 296, 305-312, 316, 317, 333, 335, 340, 346, 363, 369, 374, 378, 380, 384). Houghton and Acton observed optoacoustic signals from films of acetylene soot, camphor soot, flat-black paper, and black-body cavities (133). Marshbarger and Robin, who described an experimental configuration for optoacoustic spectroscopy in the UV and the visible region, reported its application in analyzing various solid samples--including powdered  $K_2Cr_2O_7$ , flower petals, grass, dried blood smears, ultramarine, and carbon black (118). Rosencwaig described the use of optoacoustic spectroscopy to obtain spectra for inorganic samples and biological materials (304-312). Parker (258) and Parker and Ritke (259) observed optoacoustic signals from a surface film on the window of a sample cell designed to study the collisional deactivation of singlet molecular oxygen. Bennett and Forman (33-39), Kerr (159), Kerr and Atwood (160), and Rosencwaig and Gersho (310, 311) developed not only theoretical interpretations of the optoacoustic effect observed in sample cells excited by laser or continuum sources but also theoretical explanations for the heat transfer process at the solid-gas interface. The measurement and theory of thermal diffusivity and optical absorption spectra, particularly for nonhomogeneous samples, have also been documented (14, 16, 27, 28, 33-39, 48, 52, 56, 60, 61, 69, 70, 75, 77, 80, 81, 91, 92, 94, 112, 113, 115, 118, 119, 122, 126-130, 133, 134, 155, 159, 160, 164, 166, 171, 173, 174, 177, 181-183, 185, 188, 191, 192, 195, 196, 205-208, 210-212, 217, 223, 234, 247, 256, 258, 259, 262, 265, 267, 296, 297, 300, 310, 311, 313, 316, 317-319, 330, 334-336, 340, 345, 351, 353-356, 360-362, 365, 366, 370, 372, 378, 382, 384).

One of the most recent applications of optoacoustic spectroscopy has been the detection of asbestos fibers (chrysotile) in municipal drinking water at concentrations as low as 0.1 nanograms per cubic centimeter (277). Also, the General Motors Research Laboratory has fabricated an optoacoustic spectrometer to measure diesel engine exhaust particulate emissions with a 0.5-sec response time (254, 275, 276).

In brief, according to the foregoing review of the development and application of optoacoustic spectroscopy, its use in gaseous and in solid analyses has been established and accelerated with the introduction of laser sources.

## GENERAL SYSTEM DESCRIPTION

In optoacoustic spectroscopy, radiant light energy (watts) is first converted to sound pressure (pascals), and then to an electrical potential (volts). Figure 1 represents a simplified experimental optoacoustic spectroscopy system. Light from the laser is modulated by passing it through a rotating mechanical chopper. The modulated beam then passes through a container that holds a gas sample. Energy absorbed from the laser beam heats the gas and causes its pressure to rise. Since the beam is modulated, this pressure rise is periodic at the beam modulation frequency. The periodic pressure fluctuations are detected by a microphone, converted to an electrical signal, and amplified by the pre-amplifier. The detector at the exit of the optoacoustic cell is used to sample the laser beam so that compensation can be made for variations in the optoacoustic spectra caused by wavelength and temporal intensity fluctuations of the laser emission. The two synchronized lock-in amplifiers in the signal-processing section compensate for phase changes due to laser beam walking, since a mechanical chopper with narrow slits converts beam walking to phase changes. Compensation for the aforementioned effects is accomplished by ratioing, with the ratiometer, the outputs of the lock-in amplifiers. The optoacoustic spectra are usually recorded on a strip-chart recorder for subsequent analysis.

## Acoustic Signal Generation Process

In order to maximize the sensitivity of an optoacoustic system and enhance its trace gas detection capabilities, one must understand the acoustic signal generation process and the variables affecting it.

The first step in the generation of an optoacoustic signal is the absorption of energy from the modulated laser beam. This absorbed energy produces a periodically varying heat disturbance in the gas and becomes the source of sound energy. A theoretical analysis of the acoustic signal generation process has been developed by Rosengren (313, 314) and by others (7, 8, 11, 12, 14-16, 33-35, 39, 42, 70, 77, 80, 113, 150, 152, 155, 160, 173-176, 191, 203, 204, 206, 208, 211, 212, 230-232, 240, 242, 256, 287, 306-308, 352, 354, 368). The important descriptive relationships are summarized here:

The intensity of a laser beam ( $\text{erg}\cdot\text{cm}^{-2}\cdot\text{sec}^{-1}$ ) can be expressed as  $I(\vec{r},t)$ , where  $\vec{r}$  describes position and  $t$  is time. The heat disturbance produced by the beam can be represented as  $H(\vec{r},t)$ .  $H$  has dimensions of power per unit volume ( $\text{erg}\cdot\text{cm}^{-3}\cdot\text{sec}^{-1}$ ). For many experimental situations,  $H$  and  $I$  are related by a simple proportionality constant ( $\alpha$ ):

$$H = \alpha I \quad (1)$$

The constant ( $\alpha$ ) has dimensions of reciprocal length ( $\text{cm}^{-1}$ ) and is commonly referred to as absorbance. Equation 1 is valid when the two following conditions are satisfied:

- a. The intensity ( $I$ ) is sufficiently small so that the absorbing transition is not saturated.

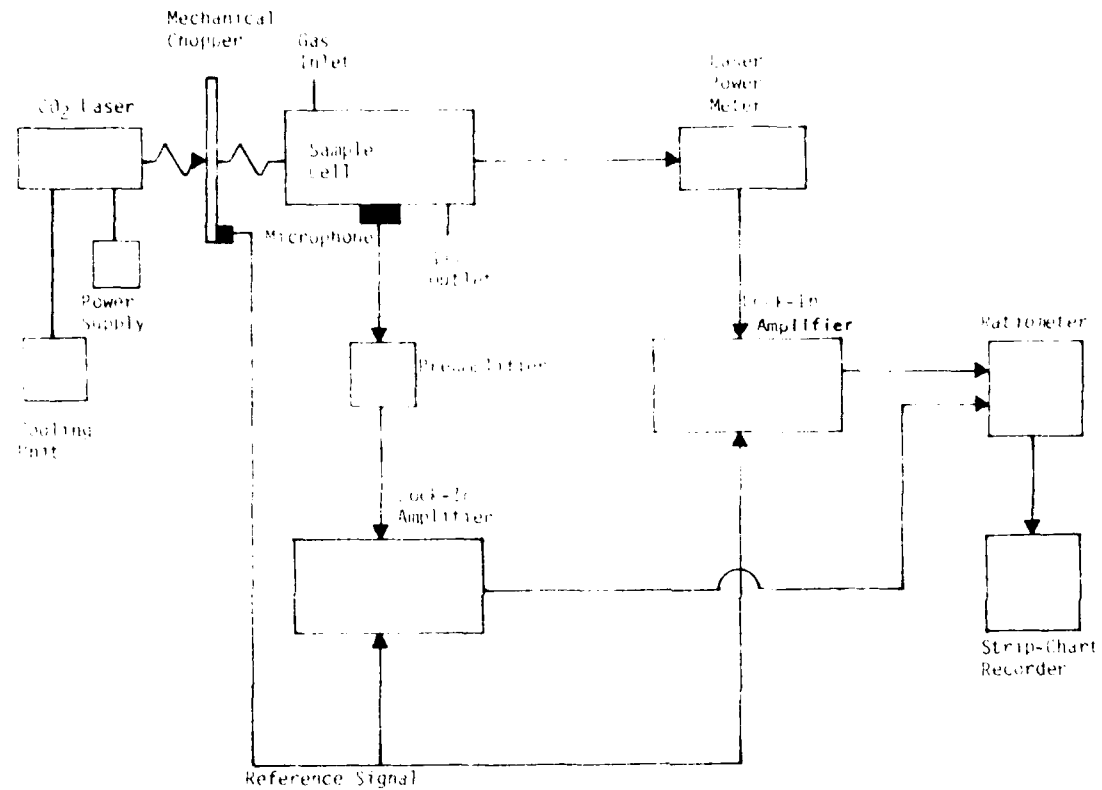


Figure 1. Optoacoustic spectrometer equipment configuration.

b. The time variation of  $I$  is much slower than the transfer rate of absorbed energy responsible for producing heat.

If either or both conditions are not satisfied, the relationship between  $I$  and  $f$  becomes complex, and quantum mechanical coherent effects must be considered. For situations when the two foregoing conditions (a and b) have been satisfied, however, a rate equation relating  $f$  and  $I$  has been developed by Kaiser (15a) and Kruezer (17a-17b).

To illustrate the rate equation, let  $N$  be the density of absorbing molecules;  $n_1$ , the density of absorbing molecules in the excited state;  $h\nu$ , the energy of the transition;  $\Delta\nu$ , the line width of the transition;  $S$ , the line strength of the transition;  $\tau_R$ , the radiative lifetime; and  $\tau_C$ , the collisional decay time of the upper state. The equation describing the upper-state population for paths of decay which are radiative and collision-induced is:

$$\frac{dn_1}{dt} = (-n_1) \left[ \frac{I}{h\nu} \left( \frac{S}{\pi\Delta\nu} \right) + \frac{\tau_C^{-1}}{\tau_R} + \tau_C^{-1} \right] + (N-n_1) \left( \frac{I}{h\nu} \right) \left( \frac{S}{\pi\Delta\nu} \right) \quad (2)$$

Under normal circumstances, collisional excitation effects in the upper state are neglected; this assumption is valid as long as  $h\nu \gg kT$ , where  $k$  is Boltzmann's constant and  $T$  is the gas temperature.

The solution of Equation 2 yields the dependence of the upper state population on light intensity ( $I$ ), density of absorbing molecules ( $N$ ), and various parameters that describe the transition. The time dependence of  $I$  can be expressed as:

$$I(t) = I_0 [1 + f(t)], \quad (3)$$

where  $I_0$  is a constant. Thus, a solution to Equation 2 is:

$$\begin{aligned} (n_1(t)/N) = & (D/F) + (2FT)^{-1} \left\{ 1 - F \exp \left\{ - \int_0^t [F + 2Df(t')] dt' \right. \right. \\ & \left. \left. \cdot \int_0^{t'} \exp \left\{ \int_0^{t''} [F + 2Df(t'')] dt'' \right\} dt' \right\} \right\} \end{aligned} \quad (4)$$

The spontaneous decay rate of the upper state ( $\tau^{-1}$ ) is given by:

$$\tau^{-1} = \tau_R^{-1} + \tau_C^{-1} \quad (5)$$

The stimulated rate ( $D$ ) for absorption or emission of radiation, is given by:

$$D = I_0 S / (\hbar v \pi \Delta v) \quad (6)$$

and the quantity  $F$  is defined as:

$$F = 2D + \tau^{-1} \quad (7)$$

The solution to Equation 2, which gives the upper-state population density, can be simplified if the time variation of  $I(t)$  is sufficiently slow. In particular, if the time variation of  $I(t)$  is slow compared to that of  $F$ , then the left side of Equation 2 can be set equal to zero. Under this condition, a solution for  $n_1$  is:

$$\frac{n_1}{N} = \frac{(IS/\hbar v \pi \Delta v)}{(2IS/\hbar v \pi \Delta v) + \tau^{-1}} \quad (8)$$

Equation 8 shows the transition saturation effect for large  $I$ , that is,  $(2IS/\hbar v \pi \Delta v \gg \tau^{-1})$ ; and in the limit of large  $I$ ,  $(n_1/N)$  becomes equal to  $(1/2)$ , and the absorbing molecules are evenly divided between the upper and lower states of the transition. In the limit for small  $I$ , Equation 8 reduces to:

$$\left(\frac{n_1}{N}\right) \approx \left(\frac{IS\tau}{\hbar v \pi \Delta v}\right) \quad (9)$$

Thus, when the time variation of  $I$  is sufficiently slow, and the intensity sufficiently weak,  $n_1$  is proportional to  $I$ .

Heat is generated in the gas by the nonradiative decay of the excited state population ( $n_1$ ). The rate of heat generation is given by:

$$H = (n_1/\tau_C) \hbar v \quad (10)$$

For those cases where Equation 8 is a good approximation, Equations 9 and 10 can be combined to yield a linear dependence of  $H$  on  $I$ . The result is:

$$\alpha = \frac{NSI}{\pi \Delta v \tau_C} \quad (11)$$

Thus, the absorbance ( $\alpha$ ) is defined as a function of the constants describing the transition process. The optoacoustic absorbance given by Equation 11 describes the conversion of light energy into heat.

The second step in the generation of the optoacoustic signal is the excitation of sound in the gas. The detailed theoretical treatment of this process has been developed by various investigators (7, 8, 11, 12, 14-16, 33-35, 39, 42, 70, 71, 80, 113, 150, 152, 155, 160, 173-176, 191, 203, 204, 206, 208, 211, 212, 230-232, 240, 256, 287, 306-308, 313, 314, 352, 354, 368). The excitation process for acoustic normal modes in a sample cell, the calculation of the quality factor for these modes, and the generation of noise by thermal fluctuations are summarized in the following:

Sound in the gas can be described by the acoustic pressure  $p(\vec{r}, t)$ , which is the difference between the total pressure  $P$ , and its average value,  $P_0$ :

$$p = P - P_0 \quad (12)$$

Morse and Ingard (228) have shown there is an acoustic velocity  $\{\vec{u}(\vec{r}, t)\}$  and temperature  $\{0(\vec{r}, t)\}$  associated with the acoustic pressure ( $p$ ). The acoustic velocity is the fluid velocity of the gas at position  $\vec{r}$  and time  $t$  caused by the sound. The acoustic temperature is the departure from the average temperature ( $T$ ) caused by the sound.

The heat  $\{H(\vec{r}, t)\}$ , produced by the absorption of light, acts as a source for the generation of sound (228). This effect can be described by:

$$\nabla^2 p - c^{-2} (\partial^2 p / \partial t^2) = - [(\gamma - 1)/c^2] (\partial H / \partial t) \quad (13)$$

where  $c$  is the velocity of sound, and  $\gamma$  is the ratio of the specific heat of the gas at constant pressure ( $C_p$ ) to that at constant volume ( $C_v$ ).

Equation 13 is an inhomogeneous wave equation that can be solved by taking the Fourier transform of both sides, and expressing the solution ( $p$ ) as an infinite series expansion of the normal mode solutions ( $p_n$ ) of the homogeneous wave equation (173, 174, 226-228, 256). The Fourier transform of Equation 13 yields:

$$(\nabla^2 + \omega^2/c^2) p(\vec{r}, \omega) = [(\gamma - 1)/c^2] i \omega H(\vec{r}, \omega) \quad (14)$$

where

$$p(\vec{r}, t) = \int p(\vec{r}, \omega) e^{-i \omega t} d\omega \quad (15)$$

$$H(\vec{r}, t) = \int H(\vec{r}, \omega) e^{-i \omega t} d\omega \quad (16)$$

The normal mode solutions for a homogeneous wave equation are determined by the boundary conditions. If the walls of the sample cell are rigid, the acoustic velocity component normal to the wall must vanish at the wall. Since the acoustic velocity ( $\dot{u}$ ) is related to the gradient of  $p$  in the following relationship ( $\rho$  is density):

$$\dot{u}(\vec{r}, \omega) = (i\omega\rho_0)^{-1} \nabla \cdot \vec{p}(\vec{r}, \omega) \quad (17)$$

it follows that the gradient of  $p$  normal to the boundary must vanish at the boundary (173, 174, 228, 256). This boundary condition determines the normal mode solutions ( $p_j$ ) of the homogeneous wave equation:

$$(\nabla^2 + k_j^2)p_j(\vec{r}) = 0 \quad (18)$$

If the resonant frequency of the normal mode ( $p_j(\vec{r})$ ) is set equal to  $\omega_j$ , these modes will be orthogonal and may be normalized with the normalization condition given by (173, 174, 226-228, 256):

$$\int p_j^* p_j dV = V_C \delta_{kj} \quad (19)$$

The volume integral is over the sample cell volume ( $V_C$ ).

For a sample cell cylinder of radius  $a$ , and length  $l$ , Equation 18 can be written in cylindrical coordinates (173, 174, 226-228, 256):

$$\vec{r}^{-1} \frac{\partial}{\partial \vec{r}} (\vec{r} \frac{\partial p_j}{\partial \vec{r}}) + \vec{r}^{-2} \frac{\partial^2 p_j}{\partial \phi^2} + \frac{\partial^2 p_j}{\partial z^2} + p_j \frac{\omega_j^2}{c^2} = 0 \quad (20)$$

Morse (226) Morse and Ingard (227, 228) found a solution given by:

$$p_j = \frac{\cos(m\phi)}{\sin(m\phi)} [A J_m(k_r \vec{r}) + B N_m(k_r \vec{r})] [C \sin(k_z z) + D \cos(k_z z)] \quad (21)$$

where  $J_m$  and  $N_m$  are Bessel functions of the first and second kind, respectively. Since  $N_m$  becomes infinite as  $\vec{r}$  approaches zero, it follows that  $B = 0$ , if Equation 20 is to represent the pressure inside a cylindrically-shaped sample

cell. To satisfy the boundary condition imposed by rigid sample cell walls, the gradient of  $p$  normal to the cell walls must vanish at the walls. If one end of the gas container is set at  $z = 0$ , and the other end is at  $z = \ell$ , it follows that  $C = 0$ , and the allowed values of  $k_z$  are given by:

$$k_z = (\pi/\ell)n_z \text{ for } (n_z = 1, 2, 3, \dots) \quad (22)$$

Applying the same boundary condition to the walls at  $\vec{r} = a$ , leads to the condition that the derivative of  $J_m(k_r \vec{r})$ , with respect to  $\vec{r}$ , must vanish at  $\vec{r} = a$ :

$$\left. \left[ \frac{d J_m(k_r \vec{r})}{d \vec{r}} \right] \right|_{\vec{r} = a} = 0 \quad (23)$$

which is equivalent to the general expression developed by Morse (226) and Morse and Ingard (227, 228):

$$\left. \left[ \frac{d J_m(\pi \alpha)}{d \alpha} \right] \right|_{\alpha = \alpha_{mn}} = 0 \quad (24)$$

$$\text{for } k_r = \pi \alpha_{mn}/a \quad (25)$$

where  $\alpha_{mn}$  is the  $n^{\text{th}}$  root of the equation involving the  $m^{\text{th}}$  order Bessel function. The requirement that  $p$  be continuous, limits  $m$  to integral values. Substituting Equation 21 into Equation 20 yields the resonant frequency of the mode:

$$\omega_j = c \left[ k_z^2 + k_r^2 \right]^{1/2} \quad (26)$$

Thus the acoustic pressure ( $p$ ) can be expressed as an expansion of the normal mode pressure components ( $p_j$ ) and their associated amplitude components ( $A_j$ ):

$$p(\vec{r}, \omega) = \sum_j A_j(\omega) p_j(\vec{r}) \quad (27)$$

Substituting Equation 27 into Equation 13 yields:

$$A_j(\omega) = - \left( \frac{i\omega}{\omega_j^2} \right) \frac{[(\gamma - 1)/V_C] \int p_j^* H dV}{(1 - \omega^2/\omega_j^2)} \quad (28)$$

which gives the mode amplitude components (173, 174, 226-228, 256). The integral in the numerator on the right side of Equation 28 represents the coupling between the heat disturbance ( $H$ ) and the normal mode pressure components ( $p_j$ ). The denominator represents the mode resonance with  $A_j$ , and becomes infinite as  $\omega$  approaches the natural resonant frequency  $\omega_j$ . This physically unreasonable situation is the result of the absence of any loss mechanism in Equation 13. A correction can be made by modifying Equation 28 to include mode damping described by the quality factor ( $Q_j$ ) (173, 174, 226-228, 256):

$$A_j(\omega) = - \left( \frac{i\omega}{\omega_j^2} \right) \frac{[(\gamma - 1)/V_C] \int p_j^* H dV}{[1 - \omega^2/\omega_j^2 - i\omega/\omega_j Q_j]} \quad (29)$$

A method for calculating  $Q_j$  from the undamped function,  $p_j$ , follows:

To show the explicit dependence of the acoustic signal on the gas absorption and light intensity,  $H$  must be replaced in Equation 29. Using Equation 1, the substitution yields:

$$A_j(\omega) = - \left( \frac{i\omega}{\omega_j^2} \right) \frac{\alpha[(\gamma - 1)/V_C] \int p_j^* I dV}{[1 - \omega^2/\omega_j^2 - i\omega/\omega_j Q_j]} \quad (30)$$

Two cases should be considered for Equation 30. First,  $I$  is assumed a constant throughout the volume of the container. In this case, the integral in the numerator of Equation 28 vanishes for  $j \neq 0$ . The lowest order mode ( $p_0$ ) has a resonant frequency ( $\omega_0 = 0$ ), and represents a constant pressure change in the container. In this particular case,  $I$  and  $p_0$  are proportional to each other, and the vanishing of the integral for  $j \neq 0$  is a direct result of the orthogonality of the functions for  $p_j$ . Under these conditions, Equation 30 reduces to:

$$A_0(\omega) = \frac{i \alpha(\gamma - 1) I}{\omega[1 + (i/\omega_T)]} \quad (31)$$

The time ( $\tau_T$ ), in the denominator of Equation 31, is the damping time for  $p_0$  resulting from heat conduction from the gas to the container walls. Assuming that the gas container is cylindrical in shape with a cross sectional area ( $A_C$ ), length ( $\ell$ ), and volume ( $V_C$ ), the total light beam power ( $W$ ) is equal to  $IV_C/\ell$ . In Equation 31 the intensity ( $I$ ) can be replaced by  $W\ell/V_C$ , to yield:

$$A_0(\omega) = \frac{i\alpha(\gamma - 1)W\ell}{\omega(1 + i/\omega\tau_0)V_C} \quad (32)$$

For the second case, the situation is considered where the spatial distribution of the intensity is adjusted so that only the first-order mode ( $p_1$ ) is excited. Equation 30 reduces to:

$$A_1(\omega) = - \left( \frac{i\omega}{\omega_1^2} \right) \frac{\alpha(\gamma - 1)W\ell}{V_C[1 - (\omega^2/\omega_1^2) - i(\omega/\omega_1)Q_1]} \quad (33)$$

Exciting a resonant mode ( $i \neq 0$ ) has distinct advantages. At low frequencies ( $\omega\tau_T \ll 1$ ), the zero-order mode amplitude is constant, is independent of frequency, and has the value:

$$A_0 = \frac{\alpha(\gamma - 1)W\ell\tau_T}{V_C} \quad (34)$$

At high frequencies ( $\omega\tau_T \gg 1$ ), the amplitude decreases as  $1/\omega$ . The first-order mode amplitude reaches a maximum at  $\omega = \omega_1$ . The ratio of the maximum amplitude of the first resonant mode to that of the zero-order mode is:

$$A_1(\omega_1)/A_0(0) = Q_1/\omega_1\tau_1 \quad (35)$$

If the value of this ratio is greater than unity, then the first-order mode amplitude is larger than the zero-mode amplitude. Thus, the value of this ratio depends on mode damping.

Calculation of the quality factor ( $Q$ ) can be accomplished by separating the viscosity and heat conduction losses into a volume and surface loss (228). The surface loss occurs in a thin region near the walls. This region can be considered to consist of two layers that extend out from the wall of the cell. One layer is of thickness  $\ell_v$ , in which the viscosity effects take place; and the

other, of thickness  $\ell_h$ , in which heat conduction effects occur. The associated skin depths are (173, 174, 226-228, 256):

$$\ell_v = 2\eta/\omega \rho_0 c_p \quad (36)$$

$$\ell_h = 2\kappa/\rho_0 \omega C_p \quad (37)$$

where  $\eta$  is the viscosity and  $\kappa$  is the thermal conductivity of the gas. The total surface loss ( $L_{sj}$ ) is given by:

$$L_{sj} = |A_j|^2 \int [1/2 R_v |\dot{u}_{tj}|^2 + 1/2 R_h |p_j|^2] dS \quad (38)$$

where  $\dot{u}_{tj}$  is the acoustic velocity component tangent to the cell's walls, and  $R_v$  and  $R_h$ , representing the loss from viscosity and heat conduction, are given by (173, 174, 226-228, 256):

$$R_v = (\eta \omega \rho_0 / 2)^{1/2} \quad (39)$$

$$R_h = [(Y - 1)/\rho_0 c^2] (\kappa \omega / 2 \rho C_p)^{1/2} \quad (40)$$

The volume loss ( $L_{vj}$ ) is given by:

$$L_{vj} = (\omega_j^2 / \rho^2 c^4) [(Y - 1)(\kappa / 2 C_p) + (2\eta / 3) |V_C| |A_j|^2] \quad (41)$$

The energy ( $E_j$ ) stored in mode  $j$  is given by:

$$E_j = V_C |A_j|^2 / \rho_0 c^2 \quad (42)$$

Therefore, the quality factor ( $Q_j$ ) can be calculated from Equations 39, 41, and 42, and the definition of  $Q$ :

$$Q_j = \omega_j \frac{\text{Energy Stored in Mode } j}{\text{Rate of Loss of Energy From Mode } j} \quad (43)$$

or

$$Q_j = \omega_j \left( \frac{E_j}{L_{sj} + L_{vj}} \right) \quad (44)$$

The acoustic normal modes of the gas-filled sample cell are also excited by thermal fluctuations, thus producing a noise source that causes a fundamental limitation on acoustic signal detection sensitivity. Kittel (165) has described the theory of thermal fluctuations. The power spectrum of the noise is given by:

$$|A_{jn}(\omega)|^2 = \frac{4\rho_0 c^2 kT}{V_C \omega_j Q_j \left\{ (1 - \omega^2/\omega_j^2)^2 + (\omega/\omega_j Q_j)^2 \right\}} \quad (45)$$

Mode damping has an influence on thermal fluctuation noise. The total energy of excitation for a mode is equal to  $kT$ , and is not affected by  $Q_j$ . However, the frequency components of the noise depend on  $Q_j$ . Increasing  $Q_j$  shifts the noise into a narrow band around the mode resonant frequency. In the case where the signal frequency is well below the mode resonant frequency ( $\omega \ll \omega_j$ ), Equation 45 reduces to:

$$|A_{jn}(\omega)|^2 = \frac{4\rho_0 c^2 kT}{\omega_j Q_j V_C} \quad (46)$$

This equation shows that noise may be reduced by increasing  $Q_j$ .

A useful quantity to evaluate the performance of a detector is the noise-equivalent-power (NEP). The NEP of an optoacoustic detector is the amount of power that would have to be absorbed by the gas to produce a signal amplitude equal to the noise amplitude given by Equation 45. For optoacoustic systems, the NEP is given by (40, 173, 174, 226-228, 256):

$$(NEP)^2 = \frac{8\pi\rho_0 c^2 kTV_C \omega^2}{\omega_j Q_j (\gamma - 1)^2} \quad (47)$$

and has the units of power (watts) per square-root of frequency (hertz). The value of Equation 47 is that it can be used to optimize the design of an opto-acoustic system. It shows that the NLP is reduced by increasing the resonant frequency and  $\Omega$ .

### Acoustic Signal Detection

The final step in the generation of an optoacoustic signal is the detection of the acoustic excitation. The detector element most commonly used is the condenser microphone. In order to calculate the magnitude of the electrical signal produced by the microphone and compensate for the noise that will be added to this signal by the microphone and its associated preamplifier, one must develop the behavioral theory of the microphone in the context of an optoacoustic application (24, 29, 80, 102, 147, 173, 174, 180, 214, 218, 219, 230, 231, 240, 242, 256, 282, 291, 309, 313, 314, 327-329, 348, 377, 386). Treatment of the condenser microphone mechanically--in terms of position, mass, damping, and spring constant--has been documented by several investigators (29, 173, 174, 180, 230, 231, 240, 256, 313, 314). Also, an electrical model of the microphone--in terms of its equivalent circuit--has been developed; and a summary of this model follows here (173, 180, 256, 328, 329, 348, 386):

The condenser microphone diaphragm is usually fabricated from a thin metal disc that is mounted to produce a large radial tension. Acoustic pressure acting on one side of the diaphragm causes it to move. This motion is detected by a change in capacity between the diaphragm and a fixed plate, mounted behind the diaphragm. Motion of the diaphragm may be described by the modes of vibration for a thin plate. Since the lowest order modes will cause the greatest change in capacity, only these modes will be considered. The motion of the diaphragm that generates a signal can be described by a single degree of freedom, which corresponds to the diaphragm bending into a spherical shape. To illustrate, consider the diaphragm at rest in the  $yz$ -plane and its center at the origin. The lowest order mode corresponds to a displacement of each point of the diaphragm in the  $x$  direction by an amount,  $x(\hat{r})$ , given by:

$$x(\hat{r}) = x(0) \left[ 1 - \hat{r}^2/b^2 \right] \quad (48)$$

where  $\hat{r}$  is the distance between the origin and any point on the diaphragm,  $x(0)$  is the displacement of the diaphragm at the origin, and  $b$  is the radius of the diaphragm. The average displacement of the diaphragm can be found by averaging  $x(\hat{r})$  over the diaphragm to yield:

$$x = (\pi b^2)^{-1} \iint x(\hat{r}) \hat{r} d\hat{r} d\theta \quad (49)$$

Substituting Equation 48 into Equation 49 yields:

$$x = 1/2 [x(0)] \quad (50)$$

that is, the average displacement is one-half the displacement at the center. The lowest order mode equation of motion for the average coordinate  $x$  is:

$$m \frac{d^2x}{dt^2} + \delta \frac{dx}{dt} + K_m x = \vec{F} \quad (51)$$

where  $m$  is the mass of the diaphragm;  $\delta$ , the damping factor;  $K_m$ , the restoring force (spring constant); and  $\vec{F}$ , the external force applied to the diaphragm. The external force has two components (a and b):

- a. the force resulting from sound pressure  $p_m A_m$ , where  $p_m$  is the average pressure over the diaphragm, and  $A_m$  is surface area of the diaphragm; and
- b. the force resulting from the microphone's bias voltage.

The force resulting from the bias voltage causes the equilibrium position of the diaphragm to shift a small amount ( $x_0$ ), which is given by:

$$x_0/d = C_m V_B^2 / d^2 K_m \quad (52)$$

where  $d$  is the distance between the diaphragm and the back plate of the microphone capacitor when the microphone is unbiased;  $C_m$  is the unbiased microphone capacitance given by:

$$C_m = \epsilon_0 A_m / d \quad (53)$$

and  $V_B$  is the microphone bias voltage.

The restoring force ( $K_m$ ) is produced by the tension ( $T_m$ ) in the microphone diaphragm:

$$K_m = 8\pi T_m \quad (54)$$

This tension must be sufficient to prevent the bias voltage from pulling the diaphragm into contact with the back plate.

The simplest and most common way to bias the condenser microphone is to apply a fixed voltage bias through a large resistor ( $R_B$ ), so that  $(R_B C_m)^{-1}$  is much less than the signal frequencies of interest. The output voltage of the microphone ( $V_s$ ) is given by:

$$V_s = p_m \frac{V_B A_m}{dK_m} \left[ 1 - \left( \frac{\omega^2}{\omega_m^2} \right) - i \left( \frac{\omega}{\omega_m Q_m} \right) \right]^{-1} \quad (55)$$

where  $\omega_m$  is the microphone resonant frequency [ $\omega_m \equiv (K_m/m)^{1/2}$ ], and  $Q_m$  is the quality factor [ $Q_m \equiv (mK_m/\delta)^{1/2}$ ]. The open-circuit voltage sensitivity ( $S_m$ ) is defined as the low-frequency ( $\omega \ll \omega_m$ ) ratio of the signal voltage ( $V_s$ ) to the sound pressure ( $p_m$ ):

$$S_m = V_B A_m / dK_m \quad (56)$$

$S_m$  in terms of the microphone equivalent volume ( $V_m$ ) is found by combining Equations 54, 55, and 56:

$$S_m = V_B V_m / dY P_0 A_m \quad (57)$$

The electrical signal generated by the microphone as a result of the opto-acoustic pressure signal can be calculated from Equation 55 by substituting the proper value for  $p_m$ . In solving Equation 13 to find  $p_m$ , one must consider the effect of the microphone on the acoustic behavior of the gas inside its container (173, 180, 256, 313, 314). The addition of the microphone to the container affects the acoustic modes of the container by changing the boundary conditions on  $p_j$ . In the absence of the microphone, the boundary conditions on the rigid container walls require that the gradient of  $p$  normal to the wall must vanish at the wall. When the microphone is added to the container, the diaphragm forms a part of the container wall and this part is no longer rigid. In this case, the boundary conditions require the acoustic velocity normal to the diaphragm surface to be equal to the diaphragm velocity ( $dx/dt$ ) produced by the acoustic pressure ( $p_m$ ), thus yielding:

$$\left[ \frac{(\nabla p)_N}{p} \right]_m = \frac{A_m}{K_m} \frac{\omega^2 p_0}{[1 - (\omega/\omega_m)^2 - i(\omega/\omega_m Q_m)]} \quad (58)$$

and  $h$  is the boundary condition at the microphone. In Equation 57,  $\langle \cos \rangle$  is the quotient of  $p$  normal to the diaphragm. When the microphone is added to the gas container, and Equation 58 is used to describe the boundary condition on  $h$ , the solutions of Equation 18 will not, in general, be orthogonal and Equations 50, 52, and 58 will not be valid. As a result, solving Equation 17 for the optoacoustic pressure becomes more complex. However, in the case for a microphone coupled to a small sample cell, a simplification can be made to reduce the complexity of this calculation.

If the container is small enough, and the modulation frequency is much less than the respective resonant frequency of the sample cell and microphone, the pressure will be constant and independent of position in the container, and the microphone will behave like an additional volume ( $V_m$ ) added to the sample cell (173, 180, 256, 313, 314). Thus,  $A_0(\omega)$  and  $V_s$  become:

$$A_0(\omega) = \frac{i\alpha(\gamma - 1)W\omega}{\omega(1+i\omega/\tau_T)(V_C + V_m)} \quad (59)$$

$$V_s = \frac{i(\lambda - 1)}{\omega \tau P_0 A_m} \left( \frac{V_B}{d} \right) \left[ \frac{V_m}{V_C + V_m} \right] (\alpha W\omega) \quad (60)$$

which gives the electrical signal produced by the microphone. These two equations describe the signal generated by an optoacoustic detector. They provide a means of evaluating the effect of design changes on signal amplitude and signal-to-noise performance.

If the dimensions of the sample cell are kept small, the first acoustic resonance mode of the combined microphone and container will occur at the modified resonant frequency of the microphone. The modified spring constant ( $K_m'$ ) can be calculated from the modified effective volume ( $V_m'$ ):

$$(V_m')^{-1} = V_m^{-1} + V_C^{-1} \quad (61)$$

$$K_m' = K_m^{-1} + V_m/V_C \quad (62)$$

The resonant frequency becomes:

$$\omega_1 = \omega_m (1 + V_m/V_C)^{1/2} \quad (63)$$

Assuming that loss comes only from microphone damping, the noise voltage  $\{ |V_{sn}(\omega)|^2 \}$  is calculated by combining Equations 46, 55, and 61-63 (where  $P_0 C^2 = \gamma P_0$ ):

$$|V_{sn}(\omega)|^2 = \left( \frac{4kT_p P_0 C'}{\omega_m Q_m V_m (1 + V_m/V_C)^2} \right) S_m^2 \quad (64)$$

An optoacoustic condenser microphone can also be modelled as a two-terminal electrical network (173, 180, 256, 327-329, 348, 386). The small signal electrical impedance of a biased microphone is identical to a series resistance-inductance-capacitance; and (RLC) resonant circuit shunted by a capacitor. An equivalent circuit is shown in Figure 2, in which  $C_m$  is the microphone high-frequency capacitance, and  $C'$ ,  $L$ , and  $R$  are determined by the restoring force, mass, and damping of the diaphragm, respectively:

$$C' = C_m^2 V_B^2 / d^2 K_m \quad (65)$$

$$L = m/K_m C' = (\omega_m^2 C')^{-1} \quad (66)$$

$$R = \delta/K_m C' = (Q_m \omega_m C')^{-1} \quad (67)$$

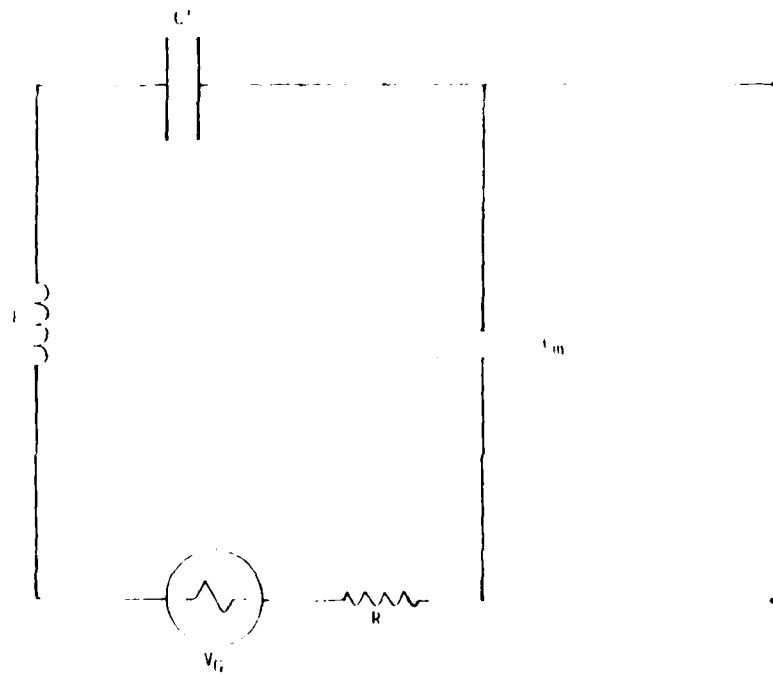


Figure 2. Condenser microphone equivalent electrical circuit.

The signal caused by an acoustic pressure ( $p_m$ ) on the diaphragm appears as a voltage ( $V_G$ ) in series with the RLC' resonant circuit, and is given by:

$$V_G = (A_m d / V_B C_m) p = (C_m / C') S_m p \quad (68)$$

where

$$C_m = \epsilon_0 A_m / d$$

In the mechanical model of the microphone, the noise appeared to be caused by viscosity and heat conduction, which resulted in a finite  $Q$ . In the electrical model, the noise is represented by the resistor Johnson noise. Johnson noise produced by the resistor in the equivalent circuit appears as a noise voltage on the output terminals, and has exactly the same amplitude as the thermal fluctuation noise. The noise at the output terminals of the microphone generated by the Johnson noise in resistor  $R$  is (40, 120, 147, 165, 197, 230, 231, 239, 242, 256, 288, 314):

$$|V_n|^2 = \frac{4kTR}{\omega^2 C_m^2} \left\{ R^2 + \left( \omega L - \frac{1 + V_m/V_C}{\omega C'} \right)^2 \right\}^{-1} \quad (69)$$

In the low-frequency limit, Equation 69 simplifies to:

$$|V_n|^2 = \frac{4kT\rho C'}{\omega_m^2 V_m (1 + V_m/V_C)^2} S_m^2 \quad (70)$$

which is identical to Equation 64.

In addition to the thermal fluctuation noise, a significant source of noise will be the microphone preamplifier (Fig. 1). Development of the theory of noise introduced by the microphone-preamplifier combination has been studied by various investigators (7, 24, 29, 78, 80, 102, 173, 174, 179, 180, 197, 229-231, 239, 256, 314, 327-329, 386). A summary of this theory follows.

The microphone electrical equivalent circuit (Fig. 2) is also useful in the development of the preamplifier noise. A model of the microphone and preamplifier equivalent circuit is shown in Figure 3. Preamplifier noise is represented by a series voltage noise source  $\{|V_{na}|^2\}$ , and a shunt current noise source  $\{|I_{nd}|^2\}$ . Noise is also generated by the Johnson noise of the bias resistor ( $R_B$ ); capacitor  $C_2$  and the associated feedback circuit are used to increase the input impedance, and thus increase the low-frequency response. Combining

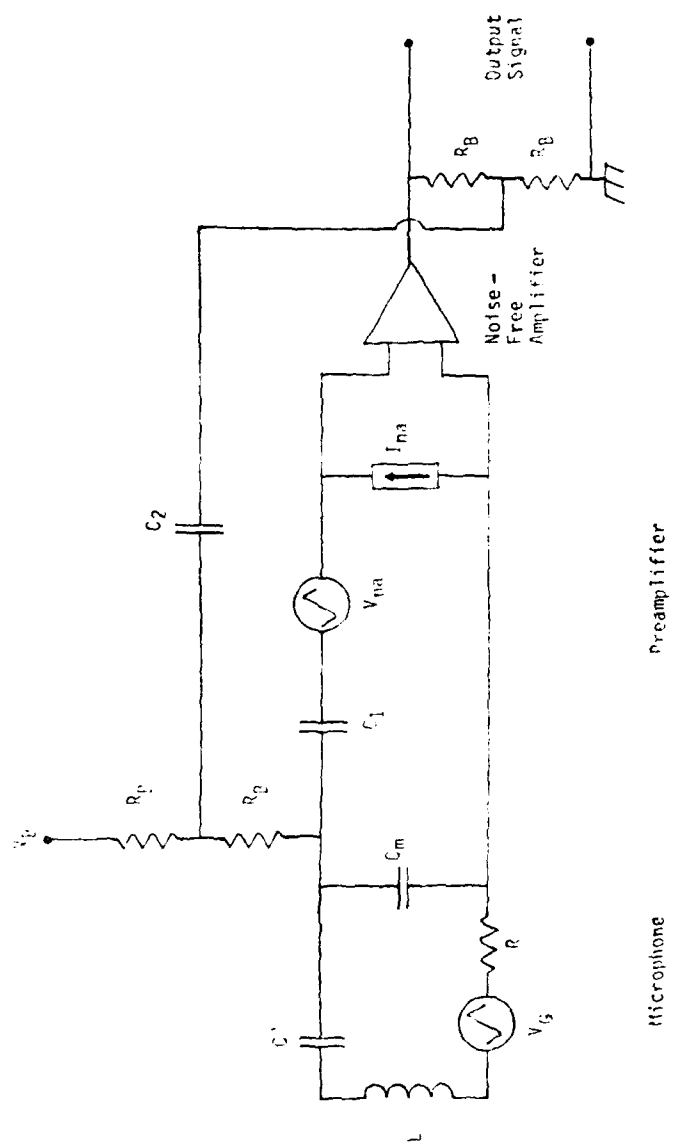


Figure 3. Condenser microphone and preamplifier equivalent electrical circuit noise model.

These three noise sources with the microphone noise yield the power spectrum  $\{V_n\}^2$  of the total noise referred to the preamplifier input:

$$\{V_n\}^2 \approx \{V_{na}\}^2 + \frac{\{I_{nd}\}^2 + 4kT/R_B}{\omega^2 C_m^2} + \frac{4KTC^4}{Q_m \omega^2 C_m^2 (1 + V_m/V_C)^2} \left[ \left( \omega^2/\omega_1^2 - 1 \right)^2 + \left( \omega/\omega_1 Q_1 \right)^2 \right]^{-1} \quad (71)$$

(7, 24, 29, 78, 80, 102, 173, 174, 179, 180, 197, 229-231, 239, 256, 314, 327-329, 386).

#### OPTIMUM DESIGN OF AN OPTOACOUSTIC SPECTROMETER TO DETECT HYDRAZINE FUELS

In designing an optoacoustic spectrometer, the optimum design will depend on the purpose of the system. The ultimate sensitivity of the system for detecting minute amounts of an absorber gas will be determined predominantly by the following six factors:

- a. the smallest absorbed power detectable by the microphone-preamplifier system,
- b. the power density of the irradiating laser beam,
- c. the signal caused by scattering and subsequent absorption of the incident laser beam by the microphone,
- d. the absorption cross section of the molecule to be detected, and
- e. the signal caused by unwanted absorption by other gas constituents (present in the environment) from which a sample is drawn for analysis.

Factors d and e are influenced by judicious selection of the absorption frequencies. This selection process requires a quantity of data about absorption spectra, laser frequencies, and possible interfering gases. The first three factors (a-c) can be optimized by employing several of the equations already developed in the previous section of this report ("Acoustic Signal Detection"). The following paragraphs present an outline that can be used for designing an optoacoustic gas spectrometer for a specific purpose.

Assume that the laser source has a fixed beam power of  $W$  watts, and that the sample cell is small enough and the modulation frequency low enough that the approximations made to derive Equations 60 and 64 are valid. The ultimate system design goal is to achieve the greatest possible absorption sensitivity (maximize the signal-to-noise ratio). The laser modulation frequency ( $\omega$ ), the dimensions of the sample cell, and the microphone design are the parameters that can readily be adjusted.

For simplicity, assume initially that the microphone preamplifier noise is insignificant compared to the combined noise of the entire system. Thus, the signal-to-noise ratio can be calculated from Equations 60 and 64 to yield:

$$\left(\frac{\text{signal}}{\text{noise}}\right)^2 = \frac{(\gamma - 1)^2}{4kT\omega^2} \left(\frac{\ell A_m}{V_C}\right)^2 \left(\frac{\omega_m Q_m}{K_m}\right) \frac{\alpha^2 W^2}{\Delta f} \quad (72)$$

The factor  $(\gamma - 1)^2$  can be increased in some situations by selecting a monatomic gas such as helium or argon, rather than nitrogen or air, to dilute the sample to be measured. However, in the case where the hydrazine fuels are diluted in air,  $\gamma$  is not adjustable. The factor  $kT$  in the denominator suggests operating the system at as low a temperature as possible. Unfortunately, condensation may prevent lowering  $T$  very much.

The factor  $(\ell A_m/V_C)^2$  can be regarded as a coupling coefficient between the microphone and the sample cell. This factor becomes large when a large area microphone and a small cross-section cell are used. For example, if the sample cell is a cylinder having length  $\ell$  and a cross-sectional area  $A_C$ , the volume is  $V_C = \ell A_C$  and the factor  $(\ell A_m/V_C)^2$  equals  $(A_m/A_C)^2$ . To maximize this factor, the smallest possible cross-sectional area is selected. This area, however, is influenced by the requirement to focus the laser beam into the container. For example, if the laser beam is of wavelength  $\lambda$  and operating in the lowest order transverse mode, then the minimum beam diameter at the ends of the gas container is achieved when the beam confocal parameter equals the cell length (79). The resultant beam radius ( $w$ ) at the input and output windows is:

$$w = (\lambda \ell / \pi)^{1/2} \quad (73)$$

The beam radius ( $w$ ) is the distance from the center of the beam at which the electric field strength is  $e^{-1}$  of its value at the beam center. The intensity at this point is  $e^{-2}$  of its value at the beam center. Selecting ( $w$ ) as the radius of the cylindrical sample cell allows most of the available laser beam power to enter the cell. The cell area becomes:

$$A_C = \lambda \ell \quad (74)$$

Substituting these results into Equation 72 yields:

$$\left(\frac{\text{signal}}{\text{noise}}\right)^2 = \frac{(\gamma - 1)^2}{4kT\omega^2} \left(\frac{A_m}{\lambda \ell}\right)^2 \frac{\alpha' W}{\delta(\Delta f)} \quad (75)$$

This equation indicates that the signal-to-noise ratio increases as the frequency is reduced. Equation 75 was derived from the assumption that  $\omega \gg \tau_f^{-1}$ . Thus, one must evaluate Equation 59 to understand the low-frequency dependence of the signal-to-noise ratio. Equation 59 indicates that the signal-to-noise ratio is maximum when the frequency is very low. Practical considerations, such as  $\tau_f^{-1}$  noise in electronics, make it more realistic to select  $\omega \approx \tau_f^{-1}$ . This choice will reduce the signal-to-noise ratio by a factor of  $\sqrt{2}$  from its ideal low-frequency limit.

The preamplifier noise was neglected in the foregoing analysis. When preamplifier noise is present, optimum system design will depend on the nature of the preamplifier noise. The signal amplitude below resonance (Eq. 60) indicates the signal amplitude can be increased by selecting a large microphone equivalent volume. The maximum signal amplitude is achieved for  $V_m \gg V_C$ . A design goal of  $V_m \approx V_C$  can readily be achieved. At low frequencies, the preamplifier current and Johnson noise from the bias resistor are the main noise sources. If the combined noise from these two noise sources is larger than the microphone fluctuation noise, the signal-to-noise ratio is independent of frequency. If the preamplifier voltage noise is sufficiently small, this frequency independence will be maintained up to the resonant frequency ( $\omega_1$ ). At this resonance, the signal-to-noise ratio is enhanced by a factor of  $Q$ . Thus, operating at resonance is desirable if the preamplifier voltage noise is small and the dominant noise source is amplifier current noise. When this source is fluctuation noise, the signal and noise are increased equally by resonance, and the optimum operating condition remains  $\omega_f \approx \tau_f^{-1}$ . Under the condition where several noise sources contribute, or  $|V_{na}|^2$  and  $|I_{na}|^2$  are not independent of frequency, the optimum operating frequency may be different from  $\tau_f^{-1}$  or  $\omega_1$  (173, 174, 180, 256).

The purpose of the following paragraphs is to utilize the absorption spectra data on the hydrazine fuels, manufacturers' equipment specifications, and the significant equations developed in this report to specify an optoacoustic spectrometer design to detect the hydrazine fuels.

#### Laser Wavelength Selection

The most convenient radiation to use in an optoacoustic system is the infrared (IR). This radiation is absorbed by many pollutants of interest at wavelengths emitted by commercially available IR lasers, and the absorption dependence on wavelength is characteristic of the molecular structure of the gas. Fortunately the bulk of air ( $N_2, O_2$ , etc.) is almost transparent to IR radiation (6, 28, 48, 52, 70, 81, 92, 107, 110, 115, 124, 152, 176, 188, 205, 263, 271, 277, 317, 318, 322, 330, 351, 356, 368, 369, 383).

The IR absorption spectra of the hydrazine fuels (hydrazine, MMH, UDME) appear in Figures 4-6. Considering the commercially available isotopic CO<sub>2</sub> lasers, the hydrazine fuel absorption spectra, and the absorption spectra of the common atmospheric constituents that could be interferences, an operating wavelength range of 10.7 to 10.9  $\mu$ m appears optimum (2, 28, 48, 59, 70, 81, 110, 124, 152, 176, 188, 221, 222, 271, 317, 318, 322-326, 351, 368, 383). The Sylvanian Model 950A sealed-tube, isotopic CO<sub>2</sub> ( $^{13}C/^{12}C$ ), 5-watt laser satisfies these requirements. The technical specifications for the laser are listed in Table 2; the tunable operating wavelengths, in Table 3; and the dimensional specifications, in Figure 7 (324-325).

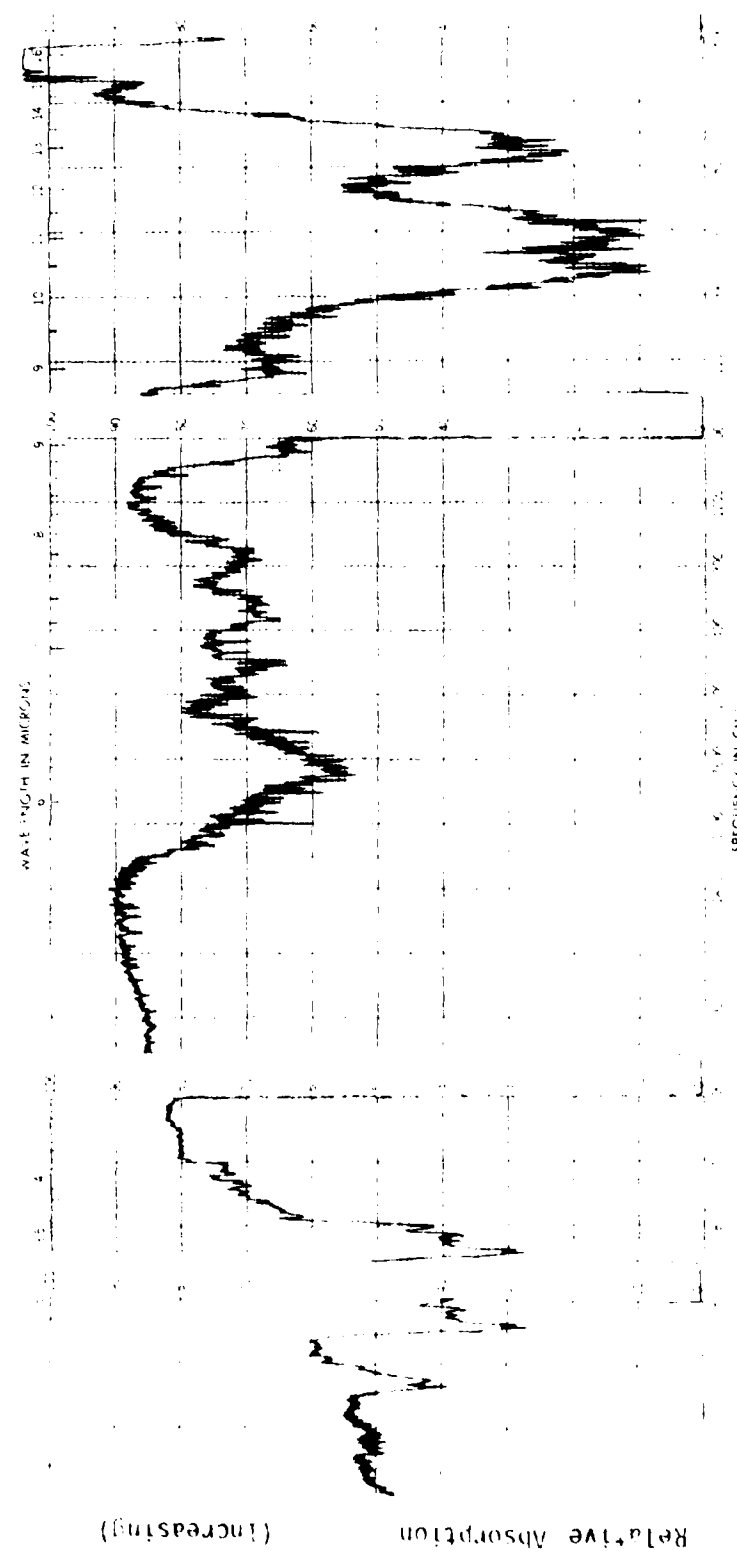


Figure 4. Hydrazine absorption spectrum.

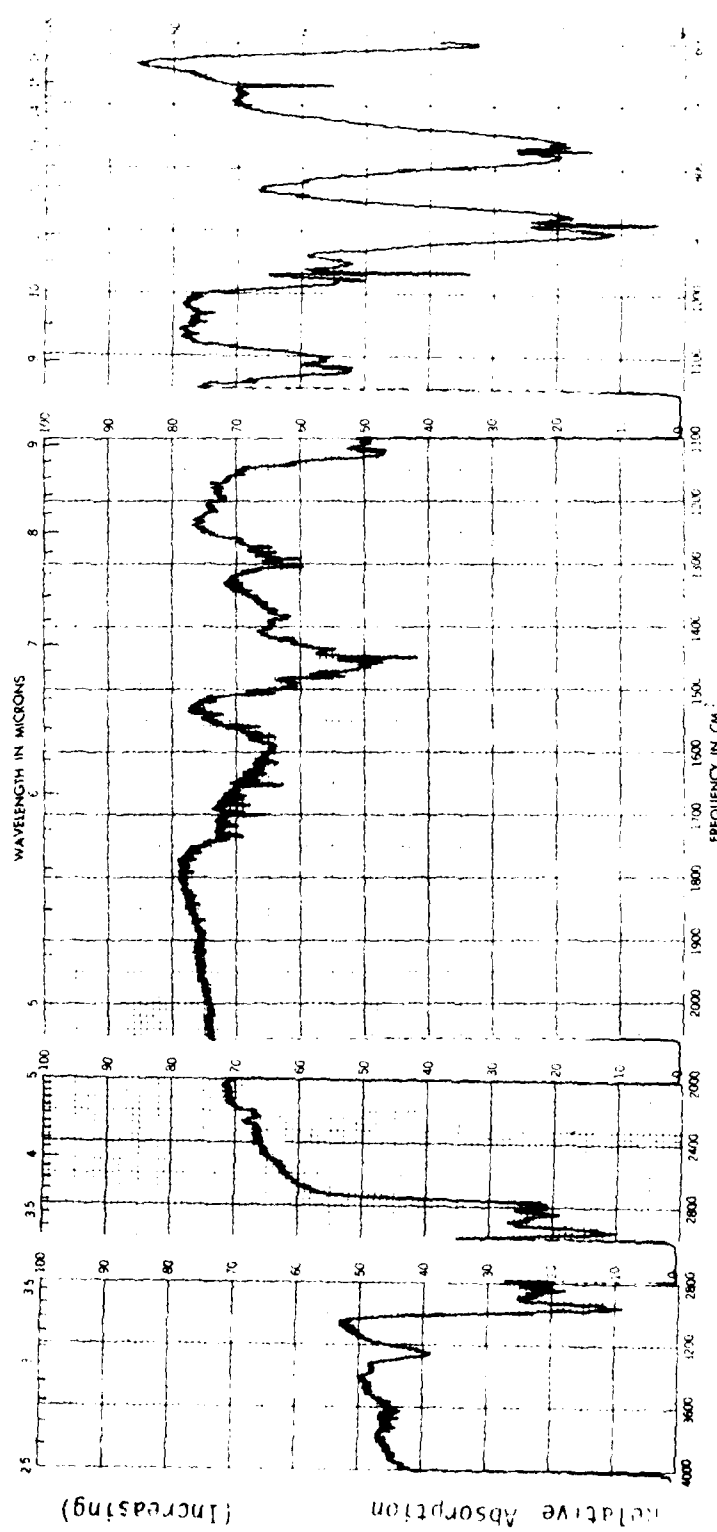


Figure 5. Monomethylhydrazine (MMH) absorption spectra.

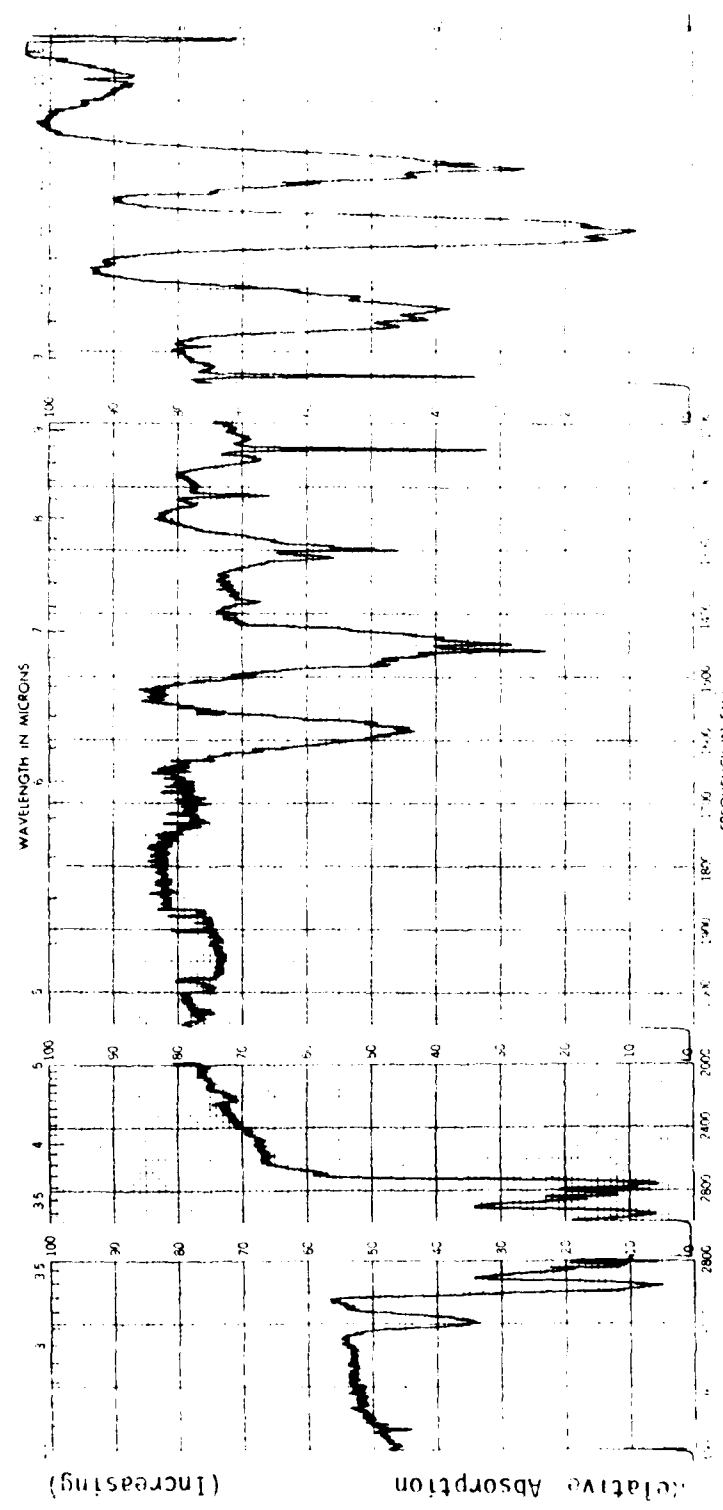


Figure 6. Absorption spectra of 1,1-dimethylhydrazine (UDMH).

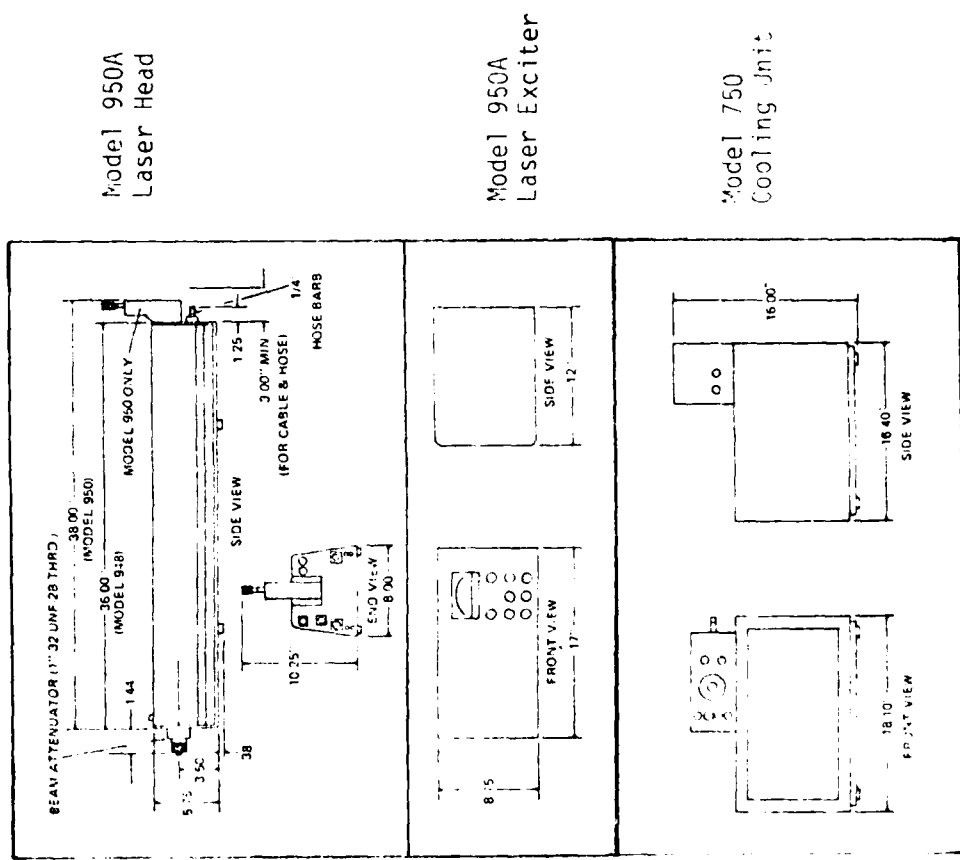


Figure 1. Dimensional specifications for the Sylvania model 950A laser head, laser exciter, and model 750 cooling unit.

TABLE 2. TECHNICAL CHARACTERISTICS OF SYLVANIA MODEL 950A CO<sub>2</sub> LASER

<u>Property</u>	<u>Value</u>
Output Wavelength (μm)	Tunable over 20 wavelengths 10.71 - 10.812 μm
Power Output	5 watts minimum at 10 or more wavelengths
Mode Purity	11 Mode
Beam Diameter (e-1 field points)	5 mm
Beam Divergence (full angle)	<3.5 mrad
Polarization (E-vector)	Vertical
Amplitude Stability	5% long-term 0.5% short-term
Frequency Stability (Long-Term: Hours)	<50 MHz (1:106); <5 MHz with Auxiliary Model 750 cooling unit
Frequency Stability (short-term: 0.1 sec)	<50 kHz (2:109)
Wavelength Selection	Calibrated In-Cavity Diffraction Grating
Optical Cavity length	77 cm
Cooling Requirements	1-4 GPM
Power Requirements	115 volts, 50/60 Hz, 600 watts
Optical Cavity Mirrors	Total Reflecting Grating 3-meter Radius of Curvature
High Voltage Source Location	Laser Head
Hardware Included	Piezoelectric Stack and Power Source, Calibrated Grating, Current Meter, Flow Switch, Interlocks, Laser Head, and Power Supply
Size: Laser Head (in.) Power Supply (in.)	6 x 8 x 38 5-1/4 x 14 x 17
Weight: Laser Head (lb) Power Supply (lb)	35 46
Warranty	1 year, including tube
Cost (Dec 79)	\$16,460
Cooling Unit	Model 750
Cooling Unit Cost (Dec 79)	\$ 1,725

TABLE 3. SYLVANIA MODEL 950A TUNABLE LASER WAVELENGTHS  
(00°1 - 10°0) BAND

Transition	Wavelength ( $\mu m$ )	Output (W)
P8	10.476	3.6
P10	10.495	5.8
P12	10.514	6.9
P14	10.533	6.9
P16	10.552	7.3
P18	10.571	7.6
P20	10.591	7.8
P22	10.612	7.7
P24	10.632	7.5
P26	10.653	7.5
P28	10.675	7.0
P30	10.697	6.4
P32	10.719	6.5
P34	10.742	5.7
P36	10.765	4.7
P38	10.788	4.3
P40	10.812	3.1
P42	10.836	2.1
R6	10.350	1.2
R8	10.333	5.4
R10	10.319	6.7
R12	10.304	7.5
R14	10.289	7.3
R16	10.275	8.1
R18	10.261	8.3
R20	10.247	8.4
R22	10.234	8.5
R24	10.220	8.3
R26	10.208	8.0
R28	10.195	7.5
R30	10.182	6.8
R32	10.171	5.8
R34	10.159	4.3

### Variable-Speed Chopper

In order to use a continuous wave (CW) laser in an optoacoustic spectrometer, the light entering the sample must be modulated. The light energy can be frequency or amplitude modulated. The preferable method is to amplitude modulate (chop) the laser light. Motor-driven slotted-wheel mechanical choppers have been designed for this purpose (87-89, 105, 108, 142, 189, 190, 278, 289). For this type of system, the actual chopping rate is determined by multiplying the number of apertures or slots in the rotating wheel by the rotational speed of the drive motor. To minimize the synchronous background signal caused by a motor-driven chopper wheel, the wheel must be balanced and vibrationally decoupled from the sample cell by means of shock-absorbing mounts. In addition, the chopper and sample cell should be spaced as far apart as possible; this step usually involves placing the chopper wheel near the laser exit window. Also desirable is minimizing the rotational velocity of the wheel by using a maximum number of apertures. McClelland and Kniseley have suggested the use of a solid chopper wheel (no slots) to reduce acoustic emission (206-208). Such a wheel could, for example, be made by depositing or photo-etching a metallic film pattern onto a fused silica disc.

Oscillatory devices, such as a tuning-fork chopper or a galvanometer-driven mirror-vane, can also be used for modulating the laser energy. However, such devices are usually limited in frequency and/or aperture.

Mechanical chopping can be avoided altogether if a pulsed laser is used. A brief investigation of this approach, however, revealed no commercial source with an acceptable combination of pulse energy and lifetime.

The mechanical variable-speed light-chopper suitable for this task is the Princeton Applied Research Model 192 Variable Speed Light Chopper. This unit has a variable chopping rate ranging from 5 to 5500 cycles/sec (Hz) (190, 278). Integrated circuitry provides dual reference signals (0 - 5 volt peak square waves) at chopping rates suitable for synchronizing the reference channels of the lock-in amplifiers that will be used in this optoacoustic spectrometer design. A brushless direct-current drive motor eliminates electrical noise caused by commutator arcing, and minimizes increases in operating temperature. Maximum temperature rise for this type of motor in continuous operation is less than 10°C, a characteristic especially important in IR work where warmer chopping blades act as an extraneous noise source. A shock-mounting plate provides mechanical isolation between the chopper motor assembly and the work surface.

### Microphone and Preamplifier

The pressure oscillation amplitudes in a sample cell can be detected with various transducers, including condenser, electret, and piezoelectric microphones (7, 20, 29, 34, 35, 39, 54, 55, 68, 77, 18, 80, 81, 96-98, 102, 114, 118, 143, 150, 152, 160, 173, 174, 179, 180, 198, 203, 204, 208, 212, 218, 219, 230, 231, 240, 256, 257, 264, 280, 287, 309, 313, 327-329, 339, 348). The condenser microphone is the most sensitive and possesses a flat frequency response in the modulation frequency range of interest for optoacoustic spectroscopy.

### Variable-Speed Chopper

In order to use a continuous wave (CW) laser in an optoacoustic spectrometer, the light entering the sample must be modulated. The light energy can be frequency or amplitude modulated. The preferable method is to amplitude modulate (chop) the laser light. Motor-driven slotted-wheel mechanical choppers have been designed for this purpose (37-89, 105, 108, 142, 189, 190, 273, 289). For this type of system, the actual chopping rate is determined by multiplying the number of apertures or slots in the rotating wheel by the rotational speed of the drive motor. To minimize the synchronous background signal caused by a motor-driven chopper wheel, the wheel must be balanced and vibrationally decoupled from the sample cell by means of shock-absorbing mounts. In addition, the chopper and sample cell should be spaced as far apart as possible; this step usually involves placing the chopper wheel near the laser exit window. Also desirable is minimizing the rotational velocity of the wheel by using a maximum number of apertures. McClelland and Kniseley have suggested the use of a solid chopper wheel (no slots) to reduce acoustic emission (206-208). Such a wheel could, for example, be made by depositing or photo-etching a metallic film pattern onto a fused silica disc.

Oscillatory devices, such as a tuning-fork chopper or a galvanometer-driven mirror-vane, can also be used for modulating the laser energy. However, such devices are usually limited in frequency and/or aperture.

Mechanical chopping can be avoided altogether if a pulsed laser is used. A brief investigation of this approach, however, revealed no commercial source with an acceptable combination of pulse energy and lifetime.

The mechanical variable-speed light-chopper suitable for this task is the Princeton Applied Research Model 192 Variable Speed Light Chopper. This unit has a variable chopping rate ranging from 5 to 5500 cycles/sec (Hz) (190, 278). Integrated circuitry provides dual reference signals (0 - 5 volt peak square waves) at chopping rates suitable for synchronizing the reference channels of the lock-in amplifiers that will be used in this optoacoustic spectrometer design. A brushless direct-current drive motor eliminates electrical noise caused by commutator arcing, and minimizes increases in operating temperature. Maximum temperature rise for this type of motor in continuous operation is less than 10°C, a characteristic especially important in IR work where warmer chopping blades act as an extraneous noise source. A shock-mounting plate provides mechanical isolation between the chopper motor assembly and the work surface.

### Microphone and Preamplifier

The pressure oscillation amplitudes in a sample cell can be detected with various transducers, including condenser, electret, and piezoelectric microphones (7, 20, 29, 34, 35, 39, 54, 55, 68, 77, 78, 80, 81, 96-98, 102, 114, 118, 143, 150, 152, 160, 173, 174, 179, 180, 198, 203, 204, 208, 212, 218, 219, 230, 231, 240, 256, 257, 264, 280, 287, 309, 313, 327-329, 339, 348). The condenser microphone is the most sensitive and possesses a flat frequency response in the modulation frequency range of interest for optoacoustic spectroscopy.

The most sensitive microphone-preamplifier combination identified from commercial sources is the Brüel & Kjaer Model 4144 air condenser microphone and Model 2619 low-noise preamplifier (63, 109, 214, 218, 219, 339). The important technical characteristics of the microphone and preamplifier are summarized in Tables 4 and 5, respectively (63, 109, 214, 218, 219, 339).

#### Laser Power Meter

A laser power meter is employed as a reference detector in the optoacoustic spectrometer shown in Figure 1. The use of this meter permits the optoacoustic signal to be normalized; and, as a result, temporal effects of laser power variations are eliminated (290). The instrument most suitable for this application is a thermopile detector (Model 210), manufactured by Coherent Radiation (184). The technical specifications for this power meter are summarized in Table 6 (184).

#### Lock-In Amplifier

The lock-in amplifier is one of the most common and effective instruments designed to measure extremely weak signal intensities in the presence of noise (1, 2, 24, 41, 44, 46, 62, 63, 66, 67, 74, 80, 90, 93, 99, 120, 131, 172, 190, 225, 230, 231, 243, 244, 278, 286, 302, 314, 337, 349, 350, 364, 385). In principle, they operate as extremely narrow-band detectors. A measurement in which a lock-in amplifier is utilized involves three main operations: amplitude modulation (AM) of a carrier wave with the desired signal information; selective amplification; and synchronous AM demodulation. The AM step is implemented at some specific point in the experimental system (e.g., chopping of laser light); and the lock-in amplifier performs the last two processing steps (1, 24, 41, 44, 46, 62, 63, 66, 74, 90, 93, 99, 120, 131, 225, 243, 244, 337, 349, 350).

The key step in a lock-in amplifier measurement (the step which gives the technique its name) is synchronous AM demodulation. Synchronous demodulation involves multiplication of the modulated carrier wave by a reference signal (chopper reference signal) which has exactly the same frequency as the carrier wave and is phase-locked to the carrier wave at zero degrees phase shift. Demodulation is completed by integrating the output of the multiplication step; this process can be accomplished using a low-pass filter.

A block diagram of a conventional lock-in amplifier is shown in Figure 8. Two input channels are provided: one to process the signal to be measured (amplitude modulated carrier); and one to process the reference signal. In almost all lock-in amplifier optoacoustic spectroscopy systems, the phase-lock reference signal is implemented by chopping the light beam with a mechanical chopper. The reference signal is then phase-locked to the carrier frequency, but is not, in general, locked at a zero degrees phase differential. Thus, a phase shifter is required in order that the relative phase of the reference signal can be adjusted with respect to the carrier signal. The comparator in the reference channel converts the reference to a bipolar square wave before this waveform is applied to the four-quadrant multiplier. Selective or tuned amplifiers are also included in each channel, and are used to exclude broad-band and discrete noise at the desired signal frequencies. The four-quadrant multiplier generates a

TABLE 4. DESIGN AND OPERATING CHARACTERISTICS OF CARTRIDGE MICROPHONE MODEL 4144  
AIRCRAFT AND MILITARY

Property	Value
Frequency response characteristic	Pressure
Open circuit frequency Response, flat within $\pm 2$ db ( $\Delta \pm 2.5$ db)	2.6 Hz to 8 kHz
Nominal Diameter	1 in.
Open circuit distortion limit (3%) db re 20 $\mu$ Pa	>148
Temperature Coefficients between $-50^{\circ}\text{C}$ and $+60^{\circ}\text{C}$ (db/ $^{\circ}\text{C}$ )	0.008
Expected long-Term stability (extrapolated)	(at $25^{\circ}\text{C}$ ) >900 years/db (at $150^{\circ}\text{C}$ ) 1.2 hour/db
Influence of static Pressure (db/atm)	-2
Influence of vibration (1 g in axial direction) db re 20 $\mu$ Pa	18
Influence of Relative humidity	<0.1 db
Height of cartridge: without protecting grid; with protecting grid	17 mm 19 mm
Diameter of Cartridge: without protecting grid; with protecting grid	23.77 mm 23.77 mm
Thread for protection grid or coupler mounting	25.17 mm - 6T NS2
Thread for preamplifier mounting	25.11 mm - 5.5 TNS2
Diaphragm Mass (kg)	$1.4 \times 10^{-5}$
Diaphragm Spring Constant (N-m $^{-1}$ )	$5.83 \times 10^4$
Diaphragm damping N - sec - m $^{-2}$	$9.24 \times 10^{-4}$
Microphone Equivalent Volume (cm $^3$ )	0.15
Open circuit Sensitivity (V-N $^{-1}$ -m $^{-2}$ )	$5 \times 10^{-2}$
High-frequency Capacitance (F)	$44 \times 10^{-12}$
Mechanical Quality Factor	0.8
Bias Voltage (V)	200
Distance Between Diaphragm and Back Plate of Condenser (m)	$2 \times 10^{-5}$
Microphone Diaphragm Area (m $^2$ )	$1.92 \times 10^{-4}$
Microphone Resonant Frequency (Hz)	$8.34 \times 10^4$

TABLE 5. TECHNICAL CHARACTERISTICS OF BRUJEL & KJAER MODEL 2019  
PREAMPLIFIER AND MODEL 2804 POWER SUPPLY

<u>Property</u>	<u>Value</u>	
Power Supply	120V/2 mA	28V/0.5 mA
	Heater 6V/60 mA	
Polarization Voltage	Transmitted through preamplifier to microphone cartridge from power supply	
Input Impedance	>10 $\Omega$ // 0.8 pF	>70 $\Omega$ // 1 pF
Output Impedance	<25 $\Omega$	<70 $\Omega$
Maximum Output Current	1.5 mA peak	0.5 mA peak
Pulse Rise Time	0.2 $\mu$ s	0.2 $\mu$ s
Pulse Decay Time	0.6 $\mu$ s	0.6 $\mu$ s
Temperature Range	-20° to + 60°C (-4° to + 140°F)	-20° to + 60°C (-4° to + 140°F)
Attenuation (Preamplifier alone)	<0.03 dB	<0.1 dB
Preamplifier Noise (dummy microphone) (Lin. 20 Hz to 200 kHz and A-weighted)		
60 pF (1 in. microphone)	<15 $\mu$ V	<2.5 $\mu$ V
17 pF (1/2 in. microphone)	<25 $\mu$ V	<4.5 $\mu$ V
6 pF (1/4 in. microphone)	<50 $\mu$ V	<15 $\mu$ V
3.5 pF (1/8 in. microphone)	<70 $\mu$ V	<25 $\mu$ V
Dimensions: Diameter:	12.7 mm (0.5 in.)	
Length:	83 mm (3.25 in.)	
Cable Length	2 m (6.6 ft)	

TABLE 6. TECHNICAL CHARACTERISTICS OF COHERENT RADIATION  
MODEL 210 LASER POWER METER

<u>Property</u>	<u>Value</u>
Detector	Thermopile
Spectral Range ( $\mu$ m)	0.3 - 30
Maximum Power Capacity (watts)	10
Rise Time ( $\mu$ sec)	1
Accuracy (per cent)	5
Active Detector Area ( $\text{mm}^2$ )	1.81
Price (Dec 79)	\$1,200

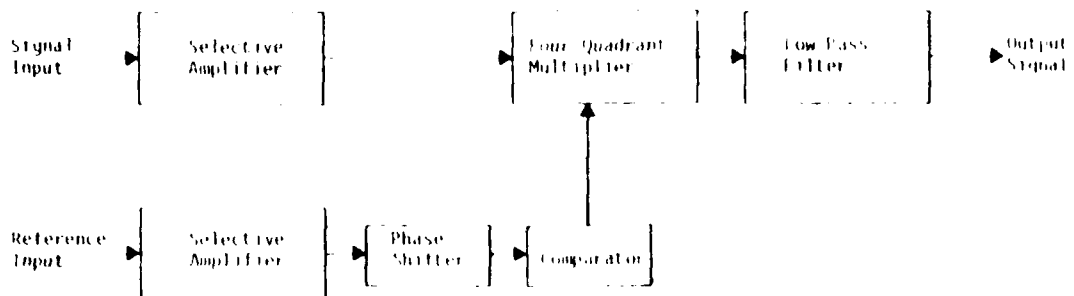


Figure 8. Conventional lock-in amplifier block diagram.

product of the phase-compensated carrier and reference signals. This multiplication process produces the desired information in a band of frequencies about the zero frequency component. Demodulation of the desired signal is completed by integrating the output of the multiplication process using a low-pass filter.

Several commercially available lock-in amplifiers are suitable for processing optoacoustic spectroscopy signals (1, 87, 88, 89, 90, 93, 138, 139, 140, 141, 142, 193, 249, 255, 280, 281, 331, 332, 341, 349, 350). These are, in general, complete processing systems and are very flexible in their application. Most of these systems merely require a direct connection to a suitable transducer (condenser microphone/preamplifier) and reference signal (mechanical chopper). A strip-chart recorder connected to the lock-in amplifier's output is convenient for producing a permanent record of the processed information. The most versatile lock-in amplifier for this optoacoustic spectrometer application is the Princeton Applied Research Corporation (PARC) Model 124A with plug-in preamplifier Model 117 (90, 93, 193, 249, 280, 281, 331, 332, 341, 350). A summary of the technical characteristics for this lock-in amplifier and preamplifier combination appears in Table 7 (90, 93, 193, 249, 280, 281, 331, 332, 341, 350).

#### Ratiometer

Compensation and normalization of laser beam temporal intensity fluctuations and phase changes can be accomplished using the configuration of lock-in amplifiers and ratiometer shown in Figure 1. (The function of the lock-in amplifiers has been discussed in the foregoing section.) Normalization of the two lock-in amplifier output signals can be accomplished with several commercially available instruments (144, 249, 290, 331, 332). The ratiometer most suitable for this optoacoustic spectrometer design is the Princeton Applied Research Corporation (PARC) Model 188 Precision Digital Ratiometer (249, 331, 332). The electrical output characteristics of this ratiometer are compatible with most laboratory strip-chart recorders. A summary of the technical specifications for the Model 188 ratiometer is presented in Table 8 (249, 331, 332).

TABLE 7. TECHNICAL CHARACTERISTICS OF PRINCETON APPLIED RESEARCH CORPORATION MODEL 124A LOCK-IN AMPLIFIER AND MODEL 117 PREAMPLIFIER

Property	Value
Frequency Range (Hz)	$2-210 \times 10^3$
Maximum Full-Scale Sensitivity (nanovolts)	100
Time Constant	1 millisecond - 300 sec (6-12 dB/octave)
Signal Channel: Modes of Filtering and Input Impedance ( $Z_{in}$ )	Modes: Notch, Flat, High-Pass, Low-Pass, and Bandpass. $Q = 1-100$ with 10 per cent Equivalent Noise Bandwidth $Z_{in} = 100$ megohms shunted by 20 picofarad capacitance
Reference Channel Modes	Internal Voltage Controlled Oscillator
Output Stability (> in 24-hour period)	15 ppm
Calibration Level	20 nanovolts to 100 millivolts in 21 levels 0.5 per cent (1 microvolt to 100 millivolts) 1 per cent (20 nanovolts to 500 nanovolts)
Price (with preamplifier) (Dec 79)	\$4,785

#### Sample Cell Design

In designing an optoacoustic system, the optimum configuration depends on the specific application. The equations presented in the preceding section of this review can be used to design an optoacoustic spectrometer to measure the hydrazine fuels.

This design will use a nonresonant, single-pass sample cell; and the microphone will be coupled directly to the gas container. The microphone and preamplifier technical characteristics appear in Tables 4 and 5 (68, 109, 214, 218, 219, 339). The laser will be operated at a wavelength of 10.812  $\mu\text{m}$ . For simplicity, the sample cell and microphone equivalent volumes are assumed equal ( $V_C = V_M$ ).

Thus the radius and length of an optimally designed nonresonant single-pass cell can be calculated from Equations 73 and 74:

$$l = (V_M/\lambda)^{1/2} = 11.78 \text{ cm} \quad (76)$$

$$w = (V_M/\pi l)^{1/2} = 6.366 \times 10^{-2} \text{ cm} \quad (77)$$

TABLE 2. TECHNICAL CHARACTERISTICS OF PRINCETON APPLIED  
RESEARCH MODEL 188 PRECISION DIGITAL RADIOMETER

<u>Property</u>	<u>Value</u>
Features	<ul style="list-style-type: none"> <li>• 4-1/2 Digit Display</li> <li>• Ratio (A/B)</li> <li>• Log Ratio (log A/B)</li> <li>• Direct Input Display of Channel A or B</li> <li>• Log of Direct Input (log A or B)</li> </ul>
Input Sensitivity	10 volts full scale for Channel A or B
Input Coupling	Direct current coupled
Input Impedance	200 kilohms
Maximum Input Voltage	> 10 volts full scale
Input Offset Voltage	> 5 microvolts per degree Centigrade
Accuracy	> 0.3 per cent average
Outputs	<ul style="list-style-type: none"> <li>• Direct Ratio Output: 10 volts full scale</li> <li>• Log Output: 1 volt per decade</li> <li>• Output Impedance: 1 kilohm</li> <li>• Output offset voltage: 100 microvolts per degree Centigrade</li> </ul>
Cost (Dec 1979)	\$1,740

The thermal damping time ( $\tau_T$ ) can be calculated by equating it to the reciprocal of the frequency at which  $\omega_h$  (given by Eq. 37) is equal to the container radius:

$$\tau_T \approx \rho_0 C_p \omega^2 / 2k \quad (78)$$

Substituting the values for air at STP [ $\rho_0 = 1.29 \times 10^{-3} \text{ gm} \cdot \text{cm}^{-3}$ ,  $C_p = 0.24 \text{ cal} (\text{gm} \cdot \text{deg})^{-1}$ , and  $k = 5.48 \times 10^{-5} \text{ cal} (\text{cm} \cdot \text{sec} \cdot \text{deg})^{-1}$ ] yields:

$$\tau_T \approx 1.145 \times 10^{-2} \text{ sec} \quad (79)$$

The noise equivalent power (NEP) can be calculated from Equation 47. Since the effective spring constant is doubled when the microphone is coupled to the gas container, it follows that  $\omega_1 Q_1 = 2 \omega_m Q_m$ . The optimum modulation frequency is  $\omega \approx \tau_T^{-1}$ . For the speed of light ( $c = 3.31 \times 10^4 \text{ cm} \cdot \text{sec}^{-1}$ ) and  $\gamma = 1.403$ , Equation 47 yields:

$$\text{NEP} = 3.6 \times 10^{-11} \text{ W}/(\text{Hz})^{1/2} \quad (80)$$

Since the absorbed power is ( $W\omega$ ), the minimum detectable absorption ( $\alpha_{\min}$ ) is:

$$\alpha_{\min} = 3.06 \times 10^{-12} \text{ W}/[\text{cm} \cdot (\text{Hz})^{1/2}] \quad (81)$$

The values of the electrical circuit elements in the equivalent circuit of Figure 2 can be calculated using the data from Tables 4 and 5. Substituting into Equation 65 yields:

$$C_m/C' = 8.7 \quad (82)$$

Therefore,

$$C' = 5.1 \times 10^{-12} \text{ farads} \quad (83)$$

When the microphone is coupled to the sample cell, the spring constant is doubled and the series capacitance ( $C'$ ) for the equivalent circuit is given by

substitution into Equation 68, where  $V_G$  is in volts and  $p_m$  is in dynes-per-square centimeter. Thus,

$$V_G = 4.4 \times 10^{-2} p_m \quad (84)$$

The values of the inductance (L) and resistance (R) are given by substitution into Equations 66 and 67. Thus,

$$L = 71 \text{ henries} \quad (85)$$

$$R = 4.68 \times 10^6 \text{ ohms} \quad (86)$$

The Johnson noise voltage generated by this resistor (R) is:

$$(4kTR)^{1/2} = 280 \text{ nanovolts}/(\text{Hz})^{1/2} \quad (87)$$

Combining Equations 84 and 87 yields the equivalent noise pressure:

$$\overline{(p_{\text{noise}}^2)}^{1/2} = 6 \times 10^{-6} \text{ dyne} \cdot \text{cm}^2/(\text{Hz})^{1/2} \quad (88)$$

If the frequency is well below resonance ( $\omega \ll \omega_1$ ), the voltage given by Equation 88 appears as a voltage at the input terminals of the preamplifier:

$$\overline{(V_{\text{nm}}^2)}^{1/2} = 29 \text{ nanovolts}/(\text{Hz})^{1/2} \quad (89)$$

In order for the preamplifier not to be the limiting noise source, the amplifier voltage and current noise must be small compared to this value, that is:

$$(\overline{|V_{\text{na}}|^2})^{1/2} < 29 \text{ nanovolts}/(\text{Hz})^{1/2} \quad (90)$$

$$(\overline{|I_{\text{na}}|^2})^{1/2} < \omega C_m (\overline{|V_{\text{nm}}|^2})^{1/2} = 10^{-16} \text{ amperes}/(\text{Hz})^{1/2} \quad (91)$$

Assuming that the current noise is produced by shot noise in the leakage current of the input field-effect transistor (FET) of the preamplifier, the leakage current,  $I_\ell$ , is restricted to:

$$I_\ell < 0.06 \times 10^{-12} \text{ amperes} \quad (92)$$

The results of the foregoing calculations are summarized in Table 9. The sample cell for a hydrazine fuel optoacoustic spectrometer is shown in Figure 9. A schematic of the optoacoustic system shows the integration of all components specified in this analysis (Fig. 10). The relative equipment costs are summarized in Table 10.

#### CONCLUSION

This analysis has presented the basic theory of optoacoustic spectroscopy oriented toward designing a specific system to measure the hydrazine fuels. The fundamental goal in designing this system has been to measure absorption with the greatest possible sensitivity and, thus, maximize the signal-to-noise ratio. In this analysis, all vital components have been selected from commercially available sources and integrated into a system design.

A word of caution is due, however, because only the fundamental sources of noise have been considered. In any real system, additional noise sources may further degrade performance. Some commonly encountered problems are extraneous acoustic noise, vibration-induced noise, and unwanted signals generated by absorption of laser beam energy by sample cell walls and windows. To fine-tune a specific system, each of these practical problems would have to be resolved. For such purposes, experimentation has yielded the best results in the past, and would be expected to do so in the future.

TABLE 9. SUMMARY OF OPTIMUM DESIGN PARAMETERS FOR A HYDRAZINE FUEL  
OPTOACOUSTIC SPECTROMETER

<u>Parameter</u>	<u>Value</u>
Sample Cell Optical Path Length ( $\ell$ )	11.78 cm
Radius of Sample Cell ( $w$ )	$6.366 \times 10^{-2}$ cm
Zero-Order Mode Damping Time ( $\tau$ )	$1.145 \times 10^{-2}$ sec
Noise Equivalent Power (NEP)	$3.6 \times 10^{-11}$ W/(Hz) <sup>1/2</sup>
Minimum Detectable Absorption ( $\alpha_{min}$ )	$3 \times 10^{-12}$ W/[cm•(Hz) <sup>1/2</sup> ]
Signal Source Voltage ( $V_G/P_m$ )	$4.4 \times 10^{-2}$ V/(dyne•cm <sup>2</sup> )
Microphone Series Resonant Capacitance ( $C_s$ )	$5.1 \times 10^{-12}$ farads
Microphone Series Resonant Inductance ( $L$ )	71 Henries
Microphone Series Resonant Resistance ( $R$ )	$4.68 \times 10^6$ ohms
Equivalent Noise Diaphragm Pressure ( $\bar{P}_n$ ) <sup>1/2</sup>	$6 \times 10^{-6}$ dyn/cm <sup>2</sup> •(Hz) <sup>1/2</sup>
Noise Voltage at Preamplifier Input Resulting from Thermal Fluctuation in Microphone and Sample Cell ( $V_{nm}$ ) <sup>1/2</sup>	29 nanovolts/(Hz) <sup>1/2</sup>
Amplifier Noise Voltage (Upper Limit) ( $\bar{V}_{na}$ ) <sup>1/2</sup>	<29 nanovolts/(Hz) <sup>1/2</sup>
Amplifier Current Noise (Upper Limit) ( $\bar{I}_{na}$ ) <sup>1/2</sup>	< $10^{-16}$ amperes/(Hz) <sup>1/2</sup>
FET Gate Leakage Current (Upper Limit) ( $I_g$ )	< $0.06 \times 10^{-12}$ amperes

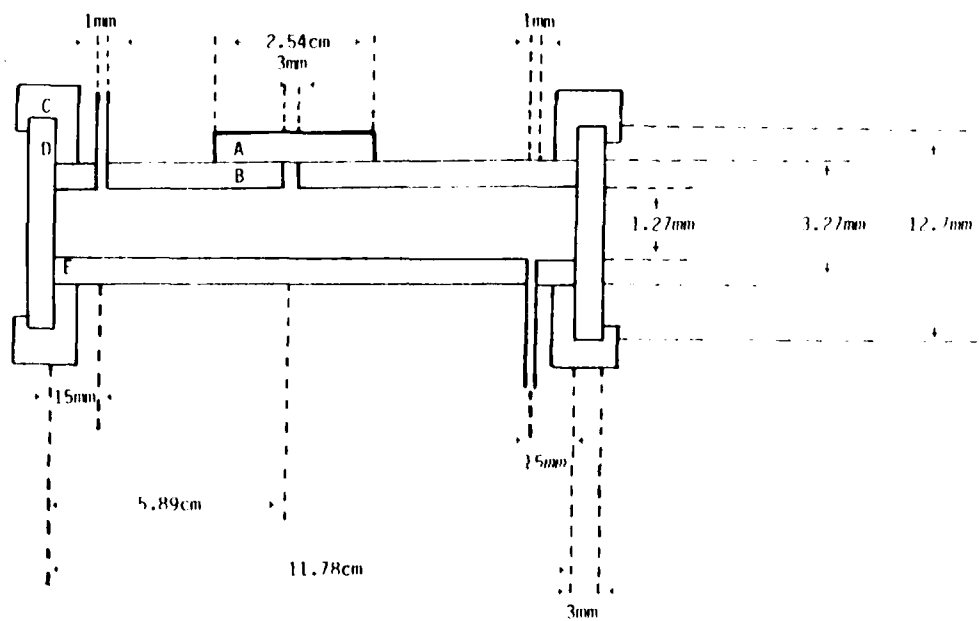


Figure 9. Nonresonant single-pass sample cell design.  
 [KEY: A = microphone,  
 B = stainless-steel sample cell,  
 C = window collar,  
 D = BaF<sub>2</sub> window, and  
 E = "O" ring seal]

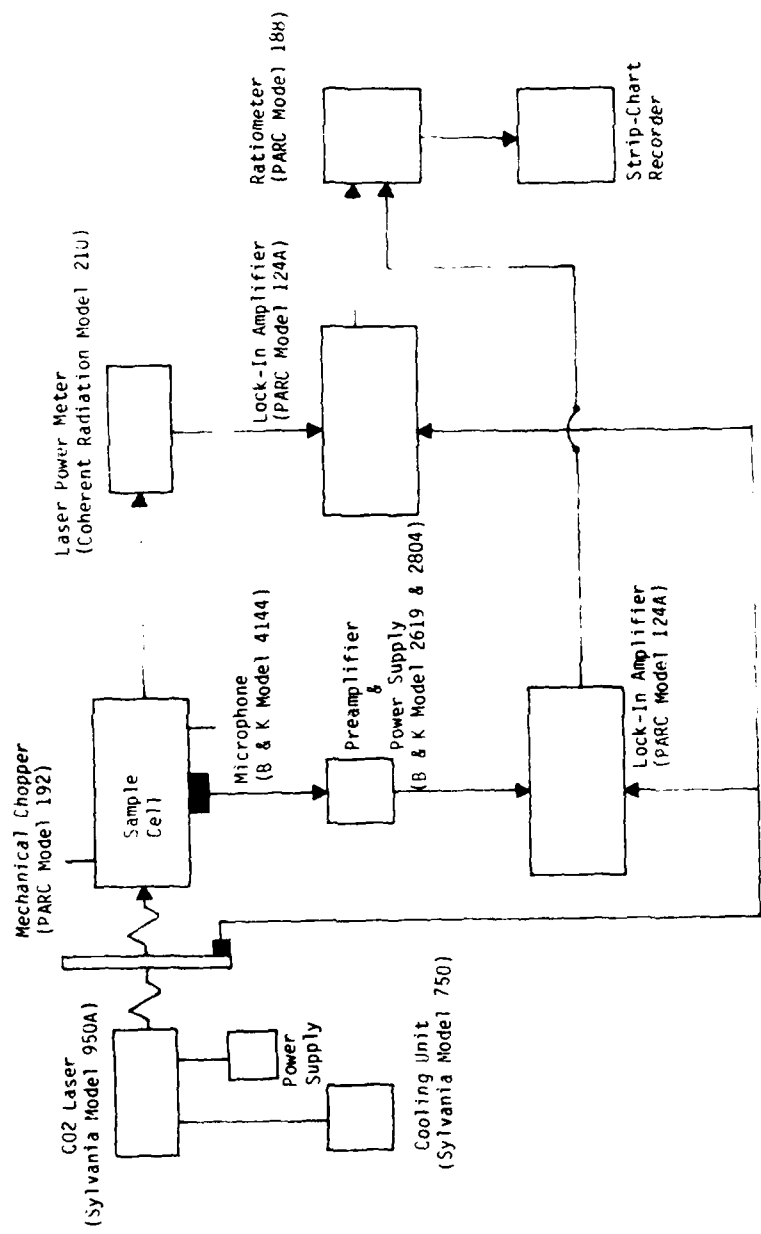


Figure 10. Optoacoustic spectrometer component integration for the measurement of the hydrazine fuels.

TABLE 10. RELATIVE ULTRASOUNDIC SPECTROMETER EQUIPMENT COSTS

<u>Component</u>	<u>Cost</u> (1979)
CO <sub>2</sub> Laser and Power Supply (Sylvania Model 950A)	\$16,480
CO <sub>2</sub> Laser Cooling Unit (Sylvania Model 750)	\$ 1,725
Variable Speed Chopper (PARC Model 192)	\$ 1,850
Microphone (Brueel & Kjaer Model 4144)	\$ 505
Microphone Preamplifier and Power Supply (Brueel & Kjaer Models 2619 & 2804)	\$ 1,173
Laser Power Meter (Coherent Radiation Model 210)	\$ 1,200
Lock-In Amplifier (PARC Model 124A; 2 Required)	\$ 9,570
Ratiometer (PARC Model 168)	\$ 1,740
Sample Cell (USAJAM Shop & Materials)	\$ 400
NET ESTIMATE (Dec 1979)	\$34,643

#### REFERENCES

1. A comparison of modern lock-in amplifiers. Bulletin 115-0175. Ithaco Incorporated, Ithaca, N.Y., 1979.
2. A practical photometric/radiometric conversion method. Application note L2009C-2. Princeton Applied Research Corporation, Princeton, N.J., 1979.
3. Aamodt, L. C., and J. C. Murphy. Photoacoustic spectroscopy of ruby powder samples. *Bull Am Phys Soc* 21:423 (1976).
4. Aamodt, L. C., J. C. Murphy, and J. G. Parker. Size considerations in the design of cells for photoacoustic spectroscopy. *J Appl Phys* 48:927 (1977).
5. Abrams, R. L., A. Yariv, and P. A. Yeh. Stark-induced three-wave mixing in molecular gases--part I: Theory. *IEEE J Quantum Elec* QE-13:79 (1977).
6. Adamowicz, R. F., and K. P. Koo. Characteristics of a photoacoustic air pollution detector at CO<sub>2</sub> laser frequencies. *Appl Opt* 18:2938 (1979).
7. Adams, M. J., A. A. King, and G. F. Kirkbright. Analytical optoacoustic spectrometry, part I. Instrument assembly and performance characteristics. *Analyst* 101:73 (1976).
8. Adams, M. J., B. C. Beadle, A. A. King, and G. F. Kirkbright. Analytical optoacoustic spectrometry, part II. Ultraviolet and visible optoacoustic spectra of some inorganic biochemical and phytochemical samples. *Analyst* 101:553 (1976).
9. Adams, M. J., B. C. Beadle, and G. F. Kirkbright. Analytical optoacoustic spectrometry, part IV. A double-beam optoacoustic spectrometer for use with solid and liquid samples in the ultraviolet, visible, and near-infrared regions of the spectrum. *Analyst* 102:569 (1977).
10. Adams, M. J., B. C. Beadle, G. F. Kirkbright, and K. R. Menon. Optoacoustic spectrometry of surfaces: dielectric coatings for laser mirrors. *Appl Spectrosc* 32:430 (1978).
11. Adams, M. J., B. C. Beadle, and G. F. Kirkbright. Optoacoustic spectrometry in the near infrared region. *Anal Chem* 50:1371 (1978).
12. Adams, M. J., and G. F. Kirkbright. Analytical optoacoustic spectrometry, part III. The optoacoustic effect and thermal diffusivity. *Analyst* 102:281 (1977).
13. Adams, M. J., and G. F. Kirkbright. Phase analysis in solid sample spectroscopy. *Spectroscopy Lett* 9:255 (1976).
14. Adams, M. J., and G. F. Kirkbright. Thermal diffusivity and thickness measurements for solid samples utilizing the optoacoustic effect. *Analyst* 102:678 (1977).

15. Adams, M. J., J. G. Highfield, and G. F. Kirkbright. Determination of absolute quantum efficiency of quinine bisulfate in aqueous medium by optoacoustic spectrometry. *Anal Chem* 49:1850 (1977).
16. Afromowitz, M. A., P. S. Yeh, and S. Yee. Photoacoustic measurements of spatially varying optical absorption in solids: a theoretical treatment. *J Appl Phys* 48:209 (1977).
17. Aggarwal, R. L., B. Lax, and G. Favrot. Noncollinear phase matching in GaAs. *Appl Phys Lett* 22:329 (1973).
18. Aggarwal, R. L., N. Lee, and B. Lax. Tunable lasers and applications. New York: Springer-Verlag, 1976.
19. Allen, J. W., R. M. MacFarlane, and R. L. White. Magnetic splittings in the optical absorption spectrum of  $\text{Cr}_2\text{O}_2$ . *Phys Rev* 179:524 (1969).
20. Amer, N. M. Method and apparatus for improved optoacoustic spectroscopy. Patent Application, filed 28 Apr 1978, 16 pp. (Available NTIS, PAT-APPL-901048/ST)
21. Angus, A. M., E. E. Marinero, and M. J. Colles. Optoacoustic spectroscopy with a visible CW dye laser. *Optics Commun* 14:223 (1975).
22. Aoki, T. Polarity of an acoustic wave produced by a switched  $\text{CO}_2$  laser. *Jap J Appl Phys* 9:1426 (1970).
23. Aoki, T., and M. Katayama. Impulsive optoacoustic effect of  $\text{CO}_2$ ,  $\text{SF}_6$ , and  $\text{NH}_3$  molecules. *Jap J Appl Phys* 10:1303 (1971).
24. Arsenault, H. H., and P. Marmet. Comparison of techniques for extracting signals from a strong background. *Rev Sci Instrum* 48:512 (1977).
25. Bagratashvili, V. N., V. P. Zharov, and V. V. Lobko. Multiple photon excitation of polyatomic molecules from the many rotational states by an intense pulse of IR radiation. *Soviet J Quantum Electronics* 8:366 (1978).
26. Bates, R. D., G. W. Flynn, and J. T. Knudtson. Laser-induced 16 micron fluorescence in  $\text{SF}_6$ : acoustic effects. *J Chem Phys* 53:3621 (1970).
27. Bauer, H. J. The optoacoustic effect in multilevel systems. *J Chem Phys* 57:3130 (1972).
28. Beck, R., W. Englisch, and K. Gurs. Table of laser lines in gases and vapors. Berlin: Springer-Verlag, 1978.
29. Becking, A. G., and A. Rodenkers. Noise in condenser microphones. *Acustica* 4:96 (1954).
30. Bell, A. G. On the production and reproduction of sound by light. *American J of Sci (Third Series)* 20:305 (1880).

31. Bell, A. G. Production and reproduction of sound by light. *Proc Am Assoc Adv Sci* 29:115 (1880).
32. Bell, A. G. Upon the production of sound by radiant energy. *Phil Mag* 11:50 (1881).
33. Bennett, H. S., and R. A. Forman. Absorption coefficients in highly transparent solids: barothermal theory. *Appl Opt* 14:3031 (1975).
34. Bennett, H. S., and R. A. Forman. Absorption coefficients of highly transparent solids: photoacoustic theory for cylindrical configurations. *Appl Opt* 15:1313 (1976).
35. Bennett, H. S., and R. A. Forman. Absorption coefficients of weakly absorbing solids: theory of a barothermal gas cell. *Appl Optics* 15:347 (1976).
36. Bennett, H. S., and R. A. Forman. Frequency dependence of photoacoustic spectroscopy: surface and bulk absorption coefficients. *J Appl Phys* 48:1432 (1977).
37. Bennett, H. S., and R. A. Forman. Measuring absorption coefficients of highly transparent solids by photoacoustic methods: cylindrical configurations. *NTIS PB253542* (1976).
38. Bennett, H. S., and R. A. Forman. Photoacoustic methods for measuring surface and bulk absorption in highly transparent materials. *Appl Opt* 15:2405 (1976).
39. Bennett, H. S., and R. A. Forman. Photoacoustic spectroscopy: a measurement technique for low absorption coefficients. *Appl Opt* 16:2834 (1977).
40. Bennett, W. R. *Electrical noise*. New York: McGraw-Hill, 1960.
41. Blair, D. P., and P. H. Sydenham. Phase sensitive detection as a means to recover signals buried in noise. *J Phys E Sci Instrum* 8:621 (1975). (Now: *J Phys [E]*)
42. Blank, R. E., and T. D. Wakefield. Double-beam photoacoustic spectrometer for use in the ultraviolet, visible, and near-infrared spectral regions. *Anal Chem* 51:50 (1979).
43. Bonczyk, P. A., and C. J. Ultee. Nitric oxide detection by use of the Zeeman-effect and CO laser. *Optics Commun* 6:196 (1972).
44. Bond, A. M., and U. S. Flego. Measurement of higher harmonics with a lock-in amplifier. *Anal Chem* 47:2321 (1975).
45. Bridges, T. J., and E. G. Burkhardt. Zeeman spectroscopy of NO with the magnetospectrophone. *Optics Commun* 22:248 (1977).
46. Brower, R. Taking noise out of weak signals. *Electronics* 41:80 (1968).

47. Bruce, C. W., B. Z. Sajka, R. J. Hurd, W. R. Watkins, K. J. White, and Z. Derzko. Application of pulsed-source spectrophone to absorption by methane at DF laser wavelengths. *Appl Opt* 15:2970 (1976).

48. Bruce, C. W., and R. G. Pinnick. In situ measurements of aerosol absorption with a resonant CW laser spectrophone. *Appl Opt* 16:1762 (1977).

49. Busse, G., and B. Bullemer. Use of the optoacoustic effect for rapid scan Fourier spectroscopy I. *Infrared Phys* 18:255 (1978).

50. Busse, G., and B. Bullemer. Use of the optoacoustic effect for rapid scan Fourier spectroscopy II. *Infrared Phys* 18:631 (1978).

51. Busse, G., and K. F. Renk. Use of the optoacoustic effect for far-infrared gas lasers. *Infrared Phys* 18:517 (1978).

52. Butler, J. F., K. W. Nill, A. W. Mantz, and R. S. Eng. Applications of tunable IR spectroscopy to chemical analyses. *Proc ACS Symp Series* No. 85, 1978.

53. Cahen, D. Photoacoustic determination of photovoltaic energy conversion. *Appl Phys Lett* 33:810 (1978).

54. Cahen, D., and H. Gaty. Sample cells for photoacoustic measurements. *Anal Chem* 51:1865 (1979).

55. Cahen, D., E. Itzak, and A. Auerbach. Simple setup for single and differential photoacoustic spectroscopy. *Rev Sci Instr* 49:1206 (1978).

56. Callis, J. B. The colorimetric detection of excited states. *J Res Nat Bur Stand (Sec A)* 80:413 (1976).

57. Castleden, S. L., C. M. Elliott, G. F. Kirkbright, and D. E. Spillane. Quantitative examination of thin-layer chromatography plates by photoacoustic spectroscopy. *Anal Chem* 51:2152 (1979).

58. Chakerian, C., and M. F. Weisbach. Amplified laser absorption: detection of nitric oxide. *J Opt Soc Am* 63:342 (1973).

59. Chang, T. Y. Accurate frequencies and wavelengths of CO<sub>2</sub> laser lines. *Optics Commun* 2:71 (1970).

60. Chappell, W. R., J. Cooper, L. W. Smith, and T. Dillon. CO<sub>2</sub> laser absorption coefficients for determining ambient levels of O<sub>3</sub>, NH<sub>3</sub>, and C<sub>2</sub>H<sub>4</sub>. *J Stat Phys* 3:401 (1971).

61. Chauanwen, C., et al. Photoacoustic spectroscopy measurements. *Laser J* 10:38 (1979).

62. Chaykowsky, D. C., and R. D. Moore. Signal-to-noise considerations in experimental research. Technical Note T-196. Princeton Applied Research Corporation, Princeton, N.J., 1968.

63. Chaykowsky, D. C., and R. D. Moore. Signal-to-noise considerations in experimental research. *Res Develop* 19:32 (1968).
64. Claspy, P. C., H. Chang, and Y. H. Pao. Optoacoustic detection of NO<sub>x</sub> using a pulsed dye laser. *Appl Opt* 16:2972 (1977).
65. Claspy, P. C., Y. H. Pao, S. Kwong, and L. Nodov. Laser optoacoustic detection of explosive vapors. *Appl Opt* 15:1506 (1976).
66. Coddington, E. G. Lock-in amplifier based on a synchronously clocked transversal filter. *Anal Chem* 51:1981 (1979).
67. Cole, J. B., and R. M. Duffy. Phase sensitive detector and reference generator for use in third derivative locking of the frequency of a laser to a saturated absorption feature. *J Phys E Sci Instrum* 7:1019 (1974). (Now: *J Phys [E]*)
68. Condenser microphone cartridges. Product data bulletin 17-253. Brüel & Kjaer Instruments, Naerum, Denmark, 1979.
69. Cottrell, T. L., I. M. MacFarlane, and A. W. Read. Measurement of vibrational relaxation times by the spectrophone. *Trans Farad Soc* 63:2093 (1969).
70. Cottrell, T. L., and J. C. McCoubrey. Molecular energy transfer in gases. London: Butterworths, 1961.
71. Crane, R. A. Laser optoacoustic absorption spectra for various explosive vapors. *Appl Opt* 17:2097 (1978).
72. Crowley, T. P., F. R. Faxvog, and D. M. Roessler. Photoacoustic effect with thermally thin solids. *Appl Phys Lett* 36:641 (1980).
73. Dailey, W. V. Proceedings of the annual analytical instrumentation symposium. New York: Plenum Press, 1967.
74. Danby, P. C. Signal recovery using a phase sensitive detector. *Elec Engr* 42:36 (1970).
75. Deaton, T. F., D. A. Depatie, and T. W. Walker. Absorption coefficient measurements of nitrous oxide and methane at DF laser wavelengths. *Appl Phys Lett* 26:300 (1975).
76. DeGroot, M. S., C. A. Emeiss, I. A. Hesselman, E. Dreut, and R. Farenhorst. Study of aldehyde photochemistry with the spectrophone technique. *Chem Phys Lett* 17:332 (1972).
77. Delaney, M. E. The optic-acoustic effect in gases. *Sci Progress* 47:459 (1959).
78. DeSmet, D. J., A. J. Jason, and A. C. Parr. Sensor/amplifier for weak light sources. NASA Technical Brief, MFS-25025, 1979.

79. Devir, A. D., and U. P. Oppenheim. Line width determination in the 9.4 micron and 10.4 micron bands of CO<sub>2</sub> using a CO<sub>2</sub> laser. *Appl Opt* 8:2121 (1969).
80. Dewey, C. F. Opto-acoustic spectroscopy. *Opt Engr* 13:483 (1974).
81. Dewey, C. F., R. D. Kamm, and C. E. Hackett. Acoustic amplifier for detection of atmospheric pollutants. *Appl Phys Lett* 23:633 (1973).
82. Dickinson, S. K. Infrared laser window materials property data for Zn, Se, KCl, NaCl, CaF<sub>2</sub>, SrF<sub>2</sub>, BaF<sub>2</sub>. NTIS AFCRL-TR-75-0318, 1975.
83. Dixon, R. N., D. A. Haner, and C. R. Webster. Optoacoustic spectroscopy with a tunable CW dye laser: forbidden transitions in some unstable sulfur compounds. *Chem Phys Lett* 22:199 (1977).
84. Douma, B. S., and T. R. Geballe. Stark cell noise reduction of a CO<sub>2</sub> laser beam. *IEEE J Quantum Elec QE-14:391* (1978).
85. Duley, W. W. CO<sub>2</sub> lasers - effects and applications. New York: Academic Press, 1976.
86. Eaton, H. E., and J. D. Stuart. Optoacoustic spectrometry of solid materials: effect of the filter gas on the observed signal. *Analyst* 102:531 (1977).
87. EG&G electro-optics condensed catalog. Princeton Applied Research Corporation, Princeton, N.J., 1978.
88. EG&G signal recovery instrumentation condensed catalog (1979-1980). Princeton Applied Research Corporation, Princeton, N.J., 1979.
89. EG&G signal recovery instrumentation domestic (USA) price list. F181C-10/79-10M-GMI, Princeton Applied Research Corporation, Princeton, N.J., 1979.
90. Engineering applications of lock-in amplifiers, application note 146, Princeton Applied Research Corporation, Princeton, N.J., 1976.
91. Ernst, M. H. Formal theory of transport coefficients to the general order in the density of gases. *Physics* 32:209 (1966).
92. Evans, L. B., H. E. Bass, and L. C. Sutherland. Atmospheric absorption of sound: theoretical predictions. *J Acoust Soc Am* 51:1565 (1972).
93. Explore the lock-in amplifier. Technical Note 115. Princeton Applied Research Corporation, Princeton, N.J., 1976.
94. Farrow, I. A., and R. F. Richton. A more complete interpretation of opto-acoustic data taken with fixed-frequency lasers. *J Appl Phys* 48:496? (1977).
95. Farrow, M. M., R. K. Burnham, and E. M. Lyring. Fourier-transform photo-acoustic spectroscopy. *Appl Phys Lett* 38:735 (1978).

96. Farrow, M. M., R. K. Burnham, M. Auzanneau, S. L. Olsen, N. Purdie, and E. M. Eyring. Piezoelectric detection of photoacoustic signals. *Appl Opt* 17:1093 (1978).
97. Farrow, M. M., R. K. Burnham, M. Auzanneau, S. L. Olsen, N. Purdie, and E. M. Eyring. Piezoelectric detection of photoacoustic signals. NTIS AD045217, 1977.
98. Fernelius, N. C., and T. W. Haas. Resonant photoacoustic cells constructed from UHV hardware. *Appl Opt* 17:3348 (1978).
99. Fisher, E. H. Lock-in amplifiers obtain measurements even if there is more noise than signal. *Laser Focus* 13:82 (1977).
100. Flynn, G. W. Lasers in chemistry. New York: Academic Press, 1974.
101. Fourier transform comes to photoacoustic spectroscopy. *Science* 208:167 (1980).
102. Fraim, F. W., and P. V. Murphy. Electrets in miniature microphones. *J Acous Soc Am* 53:1601 (1973).
103. Freed, C. Sealed-off operation of stable CO lasers. *Appl Phys Lett* 18:458 (1971).
104. Freed, C., A. H. Ross, and R. G. O'Donnell. Determination of laser line frequency and vibrational-rotational constants of the  $^{12}\text{C}^{18}\text{O}_2$ ,  $^{13}\text{C}^{16}\text{O}_2$  and  $^{13}\text{C}^{18}\text{O}_2$  isotopes from measurements of CW beat frequencies with fast HgCdTe photodiodes and microwave frequency counters. *J Mol Spectrosc* 49:439 (1974).
105. Frequency programmable variable aperture light chopper. Product bulletin. Rofin Optics and Electronics, Newton Upper Falls, Mass., 1979.
106. Freund, S. M., and D. M. Sweger. Vinyl chloride detection using carbon monoxide and carbon dioxide infrared lasers. *Anal Chem* 47:930 (1975).
107. Gelbwachs, J. Limitation to optoacoustic detection of atmospheric gases by water vapor absorption. *Appl Opt* 13:1005 (1974).
108. General Services Administration, Federal Supply Service, authorized Federal supply schedule price list. FSC group 66, part II, section L. Ithaco Incorporated, Ithaca, New York, 1979.
109. General Services Administration, Federal Supply Service, authorized Federal supply schedule supplemental price list. GSA 79/80-1. Brüel & Kjaer, Naerum, Denmark, 1979.
110. Goldan, P. D., and K. Goto. Infrared absorption in atmospheric pollutants. *J Appl Phys* 45:4350 (1974).
111. Goldberg, M. W., and R. Yusek. High-resolution inverted Lamb-dip spectroscopy on SF<sub>6</sub>. *Appl Phys Lett* 17:349 (1970).

112. Gorelik, G. A method for studying the time of energy exchange among the various degrees of freedom for gaseous molecules. *Compt Rend Acad Sci* 54:779 (1946).
113. Grabiner, F. R., D. R. Siebert, and G. W. Flynn. Laser-induced time-dependent thermal sensing studies of vibrational relaxation. *Chem Phys Lett* 17:189 (1972).
114. Gray, R. C., V. A. Fishman, and A. J. Baard. Simple sample cell for examination of solids and liquids by photoacoustic spectroscopy. *Anal Chem* 49:697 (1977).
115. Green, B. D., and J. I. Steinfeld. Absorption coefficients for fourteen gases at  $\text{CO}_2$  laser frequencies. *Appl Opt* 15:1688 (1976).
116. Griffiths, P. R., H. J. Sloane, and R. W. Hannah. Interferometers versus monochromators: separating the optical and digital advantages. *Appl Spectrosc* 31:485 (1977).
117. Hager, R. N., and R. C. Anderson. Theory of the derivative spectrometer. *J Opt Soc Am* 60:144 (1970).
118. Harshbarger, W. R., and M. B. Robin. The optoacoustic revival of an old technique for molecular spectroscopy. *Accounts of Chem Res* 6:329 (1973).
119. Hass, M., J. Davisson, H. Rosenstock, and J. Babiskin. Measurement of very low absorption coefficients by laser colorimetry. *Appl Opt* 14:1128 (1975).
120. Helstrom, C. W. Statistical theory of signal detection. London: Pergamon Press, 1968.
121. Hieftje, G. M. Signal-to-noise enhancement through instrumental techniques. *Anal Chem* 44:81A (1972).
122. Hill, D. W., and T. Powell. Non-dispersive infrared gas analysis. New York: Plenum Press, 1968.
123. Hindin, H. J. Lead-salt diode operates at room temperature. *Electronics* 53:39 (1980).
124. Hinkley, E. D., and P. L. Kelley. Detection of air pollutants with tunable diode lasers. *Science* 171:625 (1971).
125. Hocker, L. O., M. A. Kovacs, C. K. Rhodes, G. W. Flynn, and A. Jayan. Vibrational relaxation measurements in  $\text{CO}_2$  using an induced fluorescence technique. *Phys Rev Lett* 17:233 (1966).
126. Hordvik, A. Photoacoustic technique for measuring surface absorption. *J Opt Soc Am* 66:1105 (1976).

127. Hordvik, A., and H. Schlossberg. An optoacoustic technique for measuring the optical absorption coefficients in solids. *Appl Opt* 16:101 (1977).
128. Hordvik, A., and H. Schlossberg. Optoacoustic technique for measuring the optical absorption coefficient in solids. *J Opt Soc Am* 65:1165 (1976).
129. Hordvik, A., and L. Skolnik. Photoacoustic measurements of surface and bulk absorption in HF/DF laser window materials. *Appl Opt* 16:2919 (1977).
130. Hordvik, A., H. Schlossberg, H. Miller, and C. Gallagher. An optoacoustic technique for measuring the optical absorption coefficient in solids. NTIS AD 563406, RADC-TR-76-70, 1976.
131. Horlick, G., and K. R. Betty. Inexpensive lock-in amplifiers based on integrated circuit phase-locked loops. *Anal Chem* 47:363 (1975).
132. Hotta, K., K. Inove, and K. Washio. CLEOS Paper THAA4. Nippon Electric Company, Kawasaki, Japan, 1978.
133. Houghton, A. V., and R. J. Acton. Optical-acoustic effects in solid films. *AIAA J* 2:120 (1964).
134. Hunter, T. F., D. Rumbles, and M. G. Stock. Photophysical processes in vapor-phase measured by the optoacoustic effect. *J Chem Soc (Faraday II)* 70:1010 (1974).
135. Hursh, D., and T. Kuwana. Photoacoustic and spectrophotometric qualification of copper phthalocyanine films. *Anal Chem* 52:646 (1980).
136. Investigation of the absorption of infrared radiation by atmospheric gases. Aeronutronic report U-4784. Philco Ford Corporation, Aeronutronic Division, 1971.
137. Ioli, N., P. Violino, and M. Meucci. A simple transversally excited spectrophone. *J Phys [E]* 12:168 (1979). [Formerly: *J Phys F Sci Instrum*]
138. Ithaco Dynatrac 391A heterodyne lock-in amplifier. Catalog IPS-108. Ithaco Incorporated, Ithaca, N.Y., 1979.
139. Ithaco Dynatrac 393 lock-in amplifier. Catalog IPS-120. Ithaco Incorporated, Ithaca, N.Y., 1979.
140. Ithaco Dynatrac 395 lock-in amplifier. Catalog IPS-125. Ithaco Incorporated, Ithaca, N.Y., 1979.
141. Ithaco Dynatrac 397EO lock-in amplifier. Catalog IPS-132. Ithaco Incorporated, Ithaca, N.Y., 1979.
142. Ithaco instrumentation products. Short form catalog. Ithaco Incorporated, Ithaca, N.Y., 1979.

143. Ithaco low-noise preamplifiers. Catalog IPS-112. Ithaco Incorporated, Ithaca, N.Y., 1979.
144. Ithaco ratiometer-model 3512. Catalog IPS-111. Ithaco Incorporated, Ithaca, N.Y., 1979.
145. Jacobs, G. B., and H. C. Bowers. Extension of CO<sub>2</sub> laser wavelength range with isotopes. *J Appl Phys* 38:2692 (1967).
146. Jensen, R. J., and C. P. Robinson. Lasers for industrial chemistry. *Laser Focus* 16:54 (1980).
147. Johnson, J. B. Thermal agitation of electricity in conductors. *Phys Rev* 32:97 (1928).
148. Jones, P. F. Laser techniques for analysis of ambient air. Conference on Sampling and Analysis of Toxic Organics in the Atmosphere, Boulder, Colo., 5-10 August 1979.
149. Jones, R. C. The ultimate sensitivity of radiation detectors. *J Opt Soc Am* 37:879 (1947).
150. Kaiser, R. On the theory of the spectrophone. *Can J Phys* 37:1499 (1959).
151. Kaldor, A., W. B. Olson, and A. G. Maki. Pollution monitor for nitric oxide: a laser device based on the Zeeman modulation of absorption. *Science* 176:508 (1972).
152. Kamm, R. D. Detection of weakly absorbing gases using a resonant opto-acoustic method. *J Appl Phys* 47:3550 (1976).
153. Kamm, R. D., and C. F. Dewey. Proceedings of the IEEE/OSA Conference on Laser Engineering Applications, May 30 - June 1 1973, New York, 1973.
154. Kanstad, S. O., A. Bjerkestrand, and T. Lund. Tunable dual line CO<sub>2</sub> laser for atmospheric spectroscopy and pollution monitoring. *J Phys E Sci Instrum* 10:998 (1970). (Now: *J Phys [E]*)
155. Kanstad, S. O., and P. E Nordal. Infrared photoacoustic spectroscopy of solids and liquids. *Infrared Phys* 19:413 (1979).
156. Kavaya, M. J., and J. S. Margolis. Low-noise spectrophone. *NASA Technical Brief*, NPO-14362, 1979.
157. Kavaya, M. J., J. S. Margolis, and M. S. Shumate. Optoacoustic detection using stark modulation. *Appl Opt* 18:2602 (1979).
158. Kaya, K., W. R. Harschbarger, and M. B. Robin. Triplet states of biacetyl and energy transfer as revealed by optoacoustic spectroscopy. *J Chem Phys* 60:4231 (1974).
159. Kerr, E. L. The alaphone - a method for measuring thin-film absorption at laser wavelengths. *Appl Optics* 12:2520 (1973).

160. Kerr, E. L., and J. G. Atwood. The laser illuminated absorptivity spectrophone. *Appl Opt* 7:915 (1968).
161. King, A. A., and G. F. Kirkbright. Optoacoustic spectrometry for the examination of solid and semi-solid samples. *Laboratory Practice* 25:377 (1976).
162. Kingston, R. H. Detection of optical and infrared radiation. Berlin: Springer-Verlag, 1977.
163. Kirchoff, G. Über einflufs der warmeleitung in einem gase auf die schallbewegung. *Ann Phys (Leipzig)* 134:177 (1868).
164. Kisliuk, P., and C. A. Moore. Radiation from the  $^4T_2$  state of  $Cr^{3+}$  in ruby and emerald. *Phys Rev* 160:307 (1967).
165. Kittel, C. Elementary statistical physics, part 2. New York: John Wiley and Sons, 1958.
166. Knox, J. D., and Y. H. Pao. High resolution saturation spectra of the iodine isotope  $I_2^{129}$  in the 633nm wavelength region. *Appl Phys Lett* 18:360 (1971).
167. Koch, K. P., and W. Lahmann. Optoacoustic detection of sulfur dioxide below the parts-per-billion level. *Appl Phys Lett* 32:289 (1978).
168. Kogan, S. A., S. M. Luchin, and V. I. Sifrov. Valve amplifier for a spectrophone. *Compt Rend Acad Sci* 46:186 (1945).
169. Kogan, S. A., S. M. Luchin, and V. I. Sifrov. Valve amplifier for a spectrophone. *Doklady Akad Nauk* 46:204 (1945).
170. Kogelnik, H., and T. Li. Laser beams and resonators. *Appl Opt* 5:1550 (1966).
171. Kohanzadeh, Y., J. P. Whinnery, and M. M. Corroll. Thermoelastic waves generated by laser beams of low power. *J Acous Soc Am* 57:67 (1975).
172. Komachi, Y., and S. Tanaka. Lock-in amplifier using a sampled data synchronous filter. *J Phys E Sci Instrum* 8:967 (1975). [Now: *J Phys [E]*]
173. Kreuzer, L. B. Laser optoacoustic spectroscopy - a new technique of gas analysis. *Anal Chem* 46:235A (1974).
174. Kreuzer, L. B. Ultralow gas concentration infrared absorption spectroscopy. *J Appl Phys* 42:2934 (1971).
175. Kreuzer, L. B., and C. K. Patel. Nitric oxide air pollution: detection by optoacoustic spectroscopy. *Science* 173:45 (1971).
176. Kreuzer, L. B., N. B. Kenyon, and C. K. Patel. Air pollution sensitive detection of ten pollutant gases by carbon monoxide and carbon dioxide lasers. *Science* 177:347 (1972).

177. Kritchman, E., S. Shtrikman, and M. Slatkine. Resonant optoacoustic cells for trace gas analysis. *J Opt Soc Am* 68:1257 (1978).
178. Ku, R. T., E. O. Hinkley, and J. O. Sample. Long path monitoring of atmospheric carbon monoxide with a tunable diode laser system. *Appl Opt* 14:854 (1975).
179. Kuhl, W., G. R. Schodder, and F. K. Schroeder. Condenser transmitters and microphones with a solid dielectric for airborne ultrasonics. *Acustica* 4:519 (1954).
180. Kundert, W. R. Everything you have wanted to know about measurement microphones. *Sound and Vibration* 31:10 (1978).
181. Laguna, G. A., and E. Strom. Direct measurement of the absorption coefficient for transition in HF. *J Appl Phys* 46:5049 (1975).
182. Lahmann, W., H. J. Ludewig, and H. Welling. Optoacoustic trace analysis in liquids with the frequency modulated beam of an argon ion laser. *Anal Chem* 49:549 (1977).
183. Lakhov, Y. N., V. S. Mospanov, and Y. D. Fiveiskii. An optoacoustic technique for measuring the optical absorption coefficient in solids. *Sov J Quantum Elec* 1:252 (1971).
184. Laser Focus 1979 buyers' guide with fiber optic communications. Advanced Technology Publications Incorporated, Newton, Mass., 1979.
185. Lawandy, N. M. Optoacoustic measurement of vibrational-translational (V-T) rates using a short pulse CO<sub>2</sub> laser. *Infrared Phys* 20:131 (1980).
186. Lee, Y. W. Statistical theory of communications. New York: John Wiley & Sons, 1960.
187. Letzer, S. G. Explore the lock-in amplifier. *Electronic Design* 21:104 (1974).
188. Li, C. P., and J. Davis. Photoacoustic spectroscopy in several gases at CO<sub>2</sub> laser wavelengths. *Appl Opt* 18:3541 (1979).
189. Light beam chopper - model 383. Catalog IPS-110. Ithaco Incorporated, Ithaca, N.Y., 1979.
190. Light measurement terminology and techniques. Light instrumentation application note L2001A-3, Princeton Applied Research Corporation, Princeton, N.J., 1976.
191. Lin, J. W., and L. P. Dudek. Signal saturation effects and analytical techniques in photoacoustic spectroscopy of solids. *Anal Chem* 51:1627 (1979).

192. Lochmuller, C. H., S. F. Marshall, and D. R. Wilder. Photoacoustic spectroscopy of chemically bonded chromatographic stationary phases. *Anal Chem* 52:19 (1980).

193. Lock-in amplifiers. Catalog T218D-30M-12/77. Princeton Applied Research Corporation, Princeton, N.J., 1977.

194. Loper, G. L., A. R. Calloway, M. A. Stamps, and J. A. Gelbwachs. CO<sub>2</sub> laser photoacoustic detection of toxic vapors. Sixth Annual Meeting of the Federation of Analytical Chemistry and Spectroscopy Societies, Philadelphia, Pa., 16-21 Sept 1979.

195. Low, M. J., and G. A. Parodi. Infrared photoacoustic spectroscopy of solids and surface species. *Appl Spectroscopy* 34:76 (1980).

196. Luft, K. F. A new recording method for gas analysis by means of infrared absorption without spectral splitting. *Z Technische Physik* 24:97 (1943).

197. Malmstadt, H. V., C. G. Enke, S. R. Crouch, and G. Horlick. Optimization of electronic measurements. Menlo Park, Calif.: Benjamin Press, 1974.

198. Malpas, R. E., and A. J. Bard. In situ monitoring of electrochromic systems by piezoelectric detector photoacoustic spectroscopy. *Anal Chem* 52:109 (1980).

199. Mantz, A. W., E. R. Nichols, B. D. Alpert, and K. N. Rao. CO laser spectra studied with a 10 meter vacuum infrared grating spectrophotograph. *J Molecular Spectroscopy* 35:325 (1970).

200. Margolis, J. S. All electric gas detector. NASA Technical Brief, NPO-14341, 1979.

201. Margolis, J. S. Differential spectrophone. NASA Technical Brief, NPO-14599, 1979.

202. Margolis, J. S., and M. S. Schumate. Stark cell optoacoustic detection of constituent gases in a sample cell. Patent application. NASA case-NPO-14143-1 (N79-10169), serial No. 938297, 1978.

203. Maugh, T. H. Photoacoustic spectroscopy: new uses for an old technique. *Science* 188:38 (1975).

204. Max, E., and L. G. Rosengren. Characteristics of a resonant optoacoustic gas concentration detector. *Optics Commun* 11:422 (1974).

205. Mayer, A., J. Comera, H. Carpentier, and C. Jaussaud. Absorption coefficients of various pollutant gases at CO<sub>2</sub> laser wavelengths. *Appl Opt* 19:157? (1980).

206. McClelland, J. F., and R. N. Kniseley. Photoacoustic spectroscopy with condensed samples. *Appl Opt* 15:2658 (1976).

207. McClelland, J. F., and R. N. Kniseley. Scattered light effects in photo-acoustic spectroscopy. *Appl Opt* 15:2967 (1976).

208. McClelland, J. F., and R. N. Kniseley. Signal saturation effects in photoacoustic spectroscopy. *Appl Phys Lett* 28:467 (1976).

209. McCoy, J. H. Atmospheric absorption of carbon dioxide laser radiation near ten microns. Technical report 2476-2. The Ohio State University Electro-Science Laboratory, Department of Electrical Engineering, Columbus, Ohio. (Available NTIS AD839938, 1968)

210. McDavid, J. M., Y. L. Lee, S. S. Yee, and M. A. Afrumowitz. Photoacoustic determination of the optical absorptance of highly transparent solids. *J Appl Phys* 49:6112 (1978).

211. McDonald, F. A. Photoacoustic determination of small optical absorption coefficients: extended theory. *Appl Opt* 18:1363 (1979).

212. McDonald, F. A. Photoacoustic effect and the physics of waves. *Am J Phys* 48:41 (1980).

213. McFarlane, C. G., and L. D. Hess. Photoacoustic measurements of ion-implanted and laser-annealed GaAs. *Appl Phys Lett* 36:137 (1980).

214. Measuring microphones. Technical publication DK-2850. Brüel and Kjaer, Naerum, Denmark, 1972.

215. Melngailis, I., and A. Mooradian. Laser applications to optics and spectroscopy. Reading, Mass., Addison-Wesley, 1975.

216. Mercadier, M. E. Radiophony. *Phil Mag* 11:78 (1881).

217. Merkle, L. D., and R. C. Powell. Photoacoustic spectroscopy investigation of radiationless transitions in  $Eu^{2+}$  ions in KCl crystals. *Chem Phys Lett* 46:303 (1977).

218. Microphone preamplifiers. Product data bulletin 15-134. Brüel and Kjaer, Naerum, Denmark, 1978.

219. Microphones and microphone preamplifiers. Technical publication DK-2850. Brüel and Kjaer, Naerum, Denmark, 1975.

220. Model 6001 photoacoustic spectrometer. Catalog T390A-7M-8/79-RP. Princeton Applied Research Corporation, Princeton, N.J., 1979.

221. Model PL1  $CO_2$  laser. Product bulletin. Edinburgh Instruments - Boston Electronics, Boston, Mass., 1979.

222. Model PL2  $CO_2$  laser. Product bulletin. Edinburgh Instruments - Boston Electronics, Boston, Mass., 1979.

223. Monahan, E. M., and A. W. Nolle. Quantitative study of a photoacoustic system for powdered samples. *J Appl Phys* 48:3519 (1977).

224. Mooradian, A., T. Jaeger, and P. Stokseth. Tunable laser applications. Berlin: Springer-Verlag, 1977.

225. Moore, R. D. Lock-in amplifiers for signals buried in noise. *Electronics* 35:40 (1962).

226. Morse, P. M. Vibration and sound. New York: McGraw-Hill, 1948.

227. Morse, P. M., and K. V. Ingard. Encyclopedia of physics, vol XI, p. 1. Berlin: Springer-Verlag, 1961.

228. Morse, P. M., and K. V. Ingard. Theoretical acoustics. New York: McGraw-Hill, 1968.

229. Motchenbacher, C. D., and F. C. Fitchen. Low noise electronic design. New York: John Wiley and Sons, 1973.

230. Munroe, D. M., and H. S. Reichard. Photoacoustic spectroscopy of solids. Application note 147. Princeton Applied Research Corporation, Princeton, N.J., 1976.

231. Munroe, D. M., and H. S. Reichard. Practical photoacoustic spectroscopy of solids. *Am Lab* 9:119 (1977).

232. Murphy, J. C., and L. C. Aamodt. Photoacoustic spectroscopy of luminescent solids: ruby. *J Appl Phys* 48:3502 (1977).

233. Murphy, J. C., L. C. Aamodt, and C. K. Jen. Energy transport in ruby via microwave optical experiments. *Phys Rev* 314:2009 (1974).

234. Murphy, J. C., L. C. Aamodt, and C. K. Jen. Microwave induced modulation of  $R_1$  emissions in ruby above the critical concentration. *Bull Am Phys Soc* 17:109 (1972).

235. Murray, E. R., and J. E. Van Der Laan. Remote measurement of ethylene using a  $\text{CO}_2$  differential absorption lidar. *Appl Opt* 17:814 (1978).

236. Nill, K. W. Spectroscopy with tunable laser diodes. *Laser Focus* 13:32 1977.

237. Nittrover, C. A. Signal averagers. Technical application note T-162A. Princeton Applied Research Corporation, Princeton, N.J., 1968.

238. Nodov, E. Optimization of resonant cell design for optoacoustic spectroscopy (H-type). *Appl Opt* 17:1110 (1978).

239. Noise in amplifiers. Technical note 243. Princeton Applied Research Corporation, Princeton, N.J., 1976.

240. Noonan, J. A., and D. M. Munroe. What is optoacoustic spectroscopy? *Optical Spectra* 13:28 (1979).

241. Nussmeyer, T. A., and R. L. Abrams. Stark cell stabilization of a CO<sub>2</sub> laser. *Appl Phys Lett* 25:615 (1974).
242. Nyquist, H. Thermal agitation of electric charge in conductors. *Phys Rev* 32:110 (1923).
243. O'Haver, T. C. Lock-in amplifiers I. *J Chem Educ* 49:A11 (1972).
244. O'Haver, T. C. Lock-in amplifiers II. *J Chem Educ* 49:A214 (1972).
245. Oda, S., T. Sawada, and H. Kamada. Determination of ultra-trace cadmium by laser induced photoacoustic absorption spectrometry. *Anal Chem* 50:865 (1978).
246. Oda, S., T. Sawada, M. Nomura, and H. Kamada. Simultaneous determination of mixtures in liquid by laser induced photoacoustic spectroscopy. *Anal Chem* 51:686 (1979).
247. Oda, S., T. Sawada, T. Moriguchi, and H. Kamada. Analysis of turbid solutions by laser-induced photoacoustic spectroscopy. *Anal Chem* 52:650 (1980).
248. Olson, E. C., and C. D. Alway. Automatic recording of derivative ultraviolet spectra. *Anal Chem* 32:370 (1960).
249. Olson, H. F. Elements of acoustical engineering. Princeton, N.J.: Van Nostrand-Reinhold, 1947.
250. Optical elements for industry, science, and technology. Rodenstock Precision Optics Incorporated, Morton Grove, Ill., 1979.
251. Optical systems and components. Product catalog. Oriel Corporation, Stamford, Conn., 1979.
252. Optoacoustic detection. Product catalog for the model L-1400 laser optoacoustic spectrometer. Gilford Instrument Laboratories Incorporated, Oberlin, Ohio, 1979.
253. Optoacoustic spectrometer - model OAS400. Product bulletin. Rofin Optics and Electronics, Newton Upper Falls, Mass., 1979.
254. Optoacoustics measure diesel emission particulates in 0.5-sec response time. *Design News* 35:16 (1979).
255. Ortholoc SC9505. Catalog TWO 6/8. Princeton Applied Research Corporation, Princeton, N.J., 1978.
256. Pao, Y. H. Optoacoustic spectroscopy and detection. New York: Academic Press, 1977.
257. Pao, Y. H., and P. C. Claspy. Design, construction, and evaluation of a high pressure electric field optoacoustic detector. NTIS AD-A025772, 1976.

258. Parker, J. G. Optical absorption in glass: investigations using an acoustic technique. *Appl Opt* 12:2974 (1973).

259. Parker, J. G., and D. N. Ritke. Collisional deactivation of vibrationally excited singlet molecular oxygen. *J Chem Phys* 69:3713 (1973).

260. PAS-100 Photo Acoustic Cell. Data sheet PAS 241-280. Burleigh Instrumentation Company, Fishers, N.Y., 1980.

261. Patel, C. K. Coherence and quantum optics. New York: Plenum Press, 1973.

262. Patel, C. K. Use of vibrational energy transfer for excited state opto-acoustic spectroscopy of molecules. *Phys Rev Lett* 40:535 (1978).

263. Patel, C. K., E. G. Burkhardt, and C. A. Lambert. Spectroscopic measurements of stratospheric nitric oxide and water vapor. *Science* 184:1173 (1974).

264. Patel, C. K., and R. J. Kerl. A new optoacoustic cell with improved performance. *Appl Phys Lett* 30:578 (1977).

265. Patel, C. K., R. J. Kerl, and E. G. Burkhardt. Excited state spectroscopy of molecules using optoacoustic detection. *Phys Rev Lett* 38:1204 (1977).

266. Patty, R. R., G. M. Russwurm, W. A. McClenney, and D. R. Morgan. CO<sub>2</sub> laser absorption coefficients for determining ambient levels of O<sub>3</sub>, NH<sub>3</sub>, and C<sub>2</sub>H<sub>4</sub>. *Appl Opt* 13:2850 (1974).

267. Penner, S. S., K. G. Sulzmann, and H. K. Chen. Tunable laser derivative spectroscopy on spectral lines with combined doppler and collision broadening. *J Quantum Spectroscopy and Radiation Transfer* 13:705 (1973).

268. Perlmutter, P., S. Shtrikman, and M. Slatkine. Optoacoustic detection of ethylene in the presence of interfering gases. *Appl Opt* 18:2267 (1979).

269. Peterson, J. C. A differential spectrophone of unique design. Thesis, The Ohio State University, Columbus, Ohio, 1976.

270. Peterson, J. C. A study of water vapor absorption at CO<sub>2</sub> laser frequencies using a differential spectrophone and white cell. Ph.D. dissertation, The Ohio State University, Columbus, Ohio, 1978.

271. Peterson, J. C., M. E. Thomas, R. J. Nordstrom, and E. K. Damon. Water vapor-nitrogen absorption at CO<sub>2</sub> laser frequencies. *Appl Opt* 18:834 (1979).

272. Peterson, J. C., R. J. Nordstrom, and R. K. Long. Subtle source of contamination in spectrophones. *Appl Opt* 15:2974 (1976).

273. Pfund, A. H. Atmospheric contamination. *Science* 90:362 (1959).
274. Photoacoustic cell. Burleigh Instruments Incorporated product description. *Optical Spectra* 14:82 (1980).
275. Photoacoustic cell. Model PA-505 product description. Photo-Acoustics Incorporated, Rochester, Mich., 1980.
276. Photoacoustic cell. *Laser Focus* 15:73 (1979).
277. Photoacoustic observation of asbestos is described at OSA's topical meeting. *Laser Focus* 15:44 (1979).
278. Photoacoustic spectroscopy - analysis from a different point of view. Technical publication TN120-20M-2/78. Princeton Applied Research Corporation, Princeton, N.J., 1978.
279. Pidgeon, C. R., and M. J. Colles. Recent developments in tunable lasers for spectroscopy. *Nature* 279:377 (1979).
280. Preamp selection guide. Technical publication T348. Princeton Applied Research Corporation, Princeton, N.J., 1975.
281. Precision lock-in amplifier 9503. Catalog 978. Princeton Applied Research Corporation, Princeton, N.J., 1978.
282. Precision microphones for acoustic measurements. Product catalog JN996-1078. GenRad Corporation, Concord, Mass., 1979.
283. Precision optical components and precision mechanical glass work. Product catalog. Bond Optics Incorporated, Lebanon, N.H., 1979.
284. Precision optics and coatings. Product catalog. Spectra-Physics Incorporated, Mountain View, Calif., 1979.
285. Preece, W. H. On the conversion of radiant energy into sonorous vibrations. *Proc Roy Soc (London)* 31:506 (1881).
286. Price, R. The detection of signals perturbed by scatter and noise. *IRE Trans Information Theory* IT-4:163 (1954).
287. Quimby, R. S., P. M. Selzer, and W. M. Yen. Photoacoustic cell design: resonant enhancement and background signals. *Appl Opt* 16:2630 (1977).
288. Radeka, V. (1/f) noise in physical measurements. *IEEE Trans Nuclear Sci NS-16:17* (1969).
289. Radiation chopper - series 190. Product bulletin. Edinburgh Instruments - Boston Electronics, Boston, Mass., 1979.
290. Radiation measurement and control from ultraviolet to far infrared. Product catalog. Laser Precision Corporation, Utica, N.Y., 1979.

291. Rayleigh, L. The theory of sound. New York: Dover Publications, 1945.
292. Read, A. W. Impulsive optoacoustic effect of  $\text{CO}_2$ ,  $\text{SF}_6$ , and  $\text{NH}_3$  molecules. *Adv Mol Relaxation Processes* 1:257 (1967-1968).
293. Reschvkin, S. N. The theory of sound. New York: Macmillan, 1963.
294. Richton, R. E. NO line parameters measured by CO laser transmittance. *Appl Opt* 15:1686 (1976).
295. Robin, M. B., and N. A. Kuebler. Radiationless decay in the aromatic ketones as studied by optoacoustic spectroscopy. *J Am Chem Soc* 97:4822 (1975).
296. Robin, M. B., and N. A. Kuebler. Radiationless relaxation in solids as measured by a heat pulse technique. *J Chem Phys* 66:169 (1977).
297. Rockley, M. G., and J. P. Devlin. Observation of a nonlinear photoacoustic signal with potential application for nanosecond time resolution. *Appl Phys Lett* 31:24 (1977).
298. Roentgen, W. C. On tones produced by the intermittent irradiation of a gas. *Phil Mag* 11:308 (1881).
299. Roentgen, W. C. Über tone, welche durch intermittirende bestrahlung eines gases entstehen. *Ann Phyzik u Chemie* 12:155 (1881).
300. Roessler, D. M., and F. R Faxvog . Photoacoustic determination of optical absorption to extinction ratio in aerosols. *Appl Opt* 19:578 (1980).
301. Roh, W. B., and K. N. Rao. CO laser spectra. *J Mol Spectrosc* 49:317 (1974).
302. Root, W. L. An introduction to the theory of the detection of signals in noise. *Proc IEEE* 58:610 (1970).
303. Rosen, H., A. D. Hansen, L. Gundel, and T. Novakov. Photoacoustic investigation of urban aerosol particles. *Appl Opt* 17:3859 (1978).
304. Rosencwaig, A. Advances in electronics and electron physics. New York: Academic Press, 1978.
305. Rosencwaig, A. Photoacoustic spectroscopy of biological materials. *Science* 181:657 (1973).
306. Rosencwaig, A. Photoacoustic spectroscopy of solids. *Optics Commun* 7:305 (1973).
307. Rosencwaig, A. Photoacoustic spectroscopy of solids. *Phys Today* 28:23 (1975).
308. Rosencwaig, A. Photoacoustic spectroscopy of solids. *Rev Sci Instrum* 48:1133 (1977).

309. Rosencwaig, A. Photoacoustic spectroscopy: a new tool for investigation of solids. *Anal Chem* 47:592 (1975).
310. Rosencwaig, A., and A. Gersho. Photoacoustic effect with solids: a theoretical treatment. *Science* 190:556 (1975).
311. Rosencwaig, A., and A. Gersho. Theory of the photoacoustic effect with solids. *J Appl Phys* 47:64 (1976).
312. Rosencwaig, A., and J. B. Willis. Photoacoustic study of laser damage in thin films. *Appl Phys Lett* 36:667 (1980).
313. Rosengren, L. G. A new theoretical model of the optoacoustic gas concentration detector. *Infrared Phys* 13:109 (1975).
314. Rosengren, L. G. Optimal optoacoustic detector design. *Appl Opt* 14:1960 (1975).
315. Saltzman, B. E., and J. E. Cuddleback. Air pollution. *Anal Chem* 47:1R (1975).
316. Schlausener, S. A., J. D. Lindberg, and K. O. White. Differential spectrophone measurements of the absorption of laser energy by atmospheric dust. *Appl Opt* 14:2564 (1975).
317. Schlausener, S. A., J. D. Lindberg, K. O. White, and R. L. Johnson. Spectrophone measurements of infrared laser energy absorption by atmospheric dust. *Appl Opt* 15:2546 (1976).
318. Schnell, W., and G. Fischer. Carbon dioxide laser absorption coefficients of various air pollutants. *Appl Opt* 14:2058 (1975).
319. Schnell, W., and G. Fischer. Detection of air pollutants with a tunable  $\text{CO}_2$  laser. *Rapport de la Societe Suisse de Physique* 26:133 (1975).
320. Schottky, W. Über spontane stromschwankungen in verschiedenen elektrizitätsleitern. *Ann Phyzik* 57:54 (1918).
321. Schumate, M. S. Differential optoacoustic absorption detector. Patent application. NASA case-NPO-13759, serial No. 718266, 1976.
322. Schumate, M. S., R. T. Menzies, J. S. Margolis, and L. G. Rosengren. Water vapor absorption of carbon dioxide laser radiation. *Appl Opt* 15:2480 (1976).
323. Scientific laser products - sealed tube  $\text{CO}_2$  lasers and accessories. Product bulletin and price list. GTE Sylvania Incorporated, Mountain View, Calif., 1979.
324. Scientific lasers and accessories. Short form catalog. Spectra Physics Incorporated, Mountain View, Calif., 1979.

325. Series 900 CO<sub>2</sub> sealed tube lasers. Scientific laser product catalog. Spectra Physics Incorporated, Mountain View, Calif., 1979.

326. Series 3800 waveguide CO<sub>2</sub> lasers. Catalog SL3162 IM/6-79/938. Hughes Aircraft Company, Carlsbad, Calif., 1979.

327. Sessler, G. M., and J. E. West. Condenser microphones with electret foil. J Audio Eng Soc 12:129 (1964).

328. Sessler, G. M., and J. E. West. Electret transducers: a review. J Acous Soc Am 53:1589 (1973).

329. Sessler, G. M., and J. E. West. Foil-electret microphones. J Acous Soc Am 40:1433 (1966).

330. Shtrikman, S., and M. Slatkine. Trace gas analysis with a resonant opto-acoustic cell operating inside the cavity of a CO<sub>2</sub> laser. Appl Phys Lett 31:830 (1977).

331. Signal waveform recorders. Catalog T402-20M-8/79-GD. Princeton Applied Research Corporation, Princeton, N.J., 1979.

332. Signal-to-noise optimization in precision measurement systems. Technical Note T-198A. Princeton Applied Research Corporation, Princeton, N.J., 1968.

333. Skolnik, L. Optical properties of highly transparent solids. New York: Plenum Press, 1973.

334. Skolnik, L., A. Hordvik, and A. Kahan. Laser doppler interferometry for measuring small absorption coefficients. Appl Phys Lett 23:477 (1973).

335. Skomoano, R. Photoacoustic spectroscopy of condensed matter. Angew Chem Int'l Ed Engl 17:238 (1978).

336. Slobodskaya, P. V. Determination of the velocity of the transition from vibrational to translational energy of molecules with the aid of a spectrophone. Izvest Akad Nauk 12:656 (1948).

337. Smith, K. L. The ubiquitous phase detector. Wireless World 77:367 (1972).

338. Smith, R. G. Laser handbook. Amsterdam: North Holland Publications, 1972.

339. Sound, vibration, and signal analysis instrumentation. Short form catalog. Brüel & Kjaer, Naerum, Denmark, 1979.

340. Sparks, M., and C. J. Duthler. Theory of infrared absorption and material failure in crystals inclusions. J Appl Phys 44:3033 (1973).

341. Specifying lock-in amplifiers. Technical Note 116. Princeton Applied Research Corporation, Princeton, N.J., 1976.

342. Spencer, D. J., G. C. Denault, and H. H. Takimoto. Atmospheric gas absorption at DF laser wavelengths. *Appl Opt* 13:2855 (1974).

343. Steinfeld, J. I., and B. D. Green. Monitoring spacecraft atmospheric contaminants by laser absorption spectroscopy. NASA final technical report NGR-22-009-766, 1976.

344. Steinfeld, J. I., and C. C. Jensen. Tunable lasers applications. Berlin: Springer-Verlag, 1976.

345. Stepanov, B. I., and O. P. Girrin. Determination of the duration of the excited oscillatory state with the aid of the spectrophone. *J Exptl Theor Phys (USSR)* 20:947 (1950).

346. Swada, T., S. Oda, H. Shimizu, and H. Kamada. Laser-induced photoacoustic spectroscopy of some rare earth ions in aqueous solutions. *Anal Chem* 51:688 (1978).

347. Sweger, D. M., and J. C. Travis. An application of infrared lasers to the selective detection of trace organic gases. *Appl Spectrosc* 33:46 (1979).

348. Terr, K. On the optimum configuration for a condenser microphone. *Acustica* 15:256 (1965).

349. The heterodyning lock-in amplifier. Catalog IAN-23. Ithaco Incorporated, Ithaca, N.Y., 1979.

350. The use of a lock-in amplifier for the detection and measurement of light signals. Special signal application note. Princeton Applied Research Corporation, Princeton, N.J., 1967.

351. Thomas, L. J., M. J. Kelley, and N. M. Amer. The role of buffer gases in optoacoustic spectroscopy. *Appl Phys Lett* 32:736 (1978).

352. Thurston, R. N. Physical acoustics. New York: Academic Press, 1964.

353. Tolstoi, N. A., L. Shun-fu, and M. E. Lapidus. The luminescence kinetics of chromium lumens. *Opt Spectrosc (USSR)* 13:133 (1962).

354. Tripodi, R. Interpretation of spectrophone results for  $\text{CO}_2$ . *J Chem Phys* 52:3298 (1970).

355. Tripodi, R., and W. G. Vincenti. A gas dynamic model for coupled vibrational and radiative nonequilibrium in  $\text{CO}_2$  with an application to the spectrophone. *J Chem Phys* 55:2207 (1971).

356. Trusty, G. L. Absorption measurements of the 10.4 micron region using a  $\text{CO}_2$  laser and a spectrophone. NTIS AD 907549, 1972.

357. Tyndall, J. Action of an intermittent beam of radiant heat upon gaseous matter. *Proc Roy Soc (London)* 31:307 (1881).

358. Ultraviolet, visible, infrared lens systems. General catalog. Unique Optical Company, Farmingdale, N.Y., 1979.

359. Van Der Ziel, A. Noise. Englewood-Cliffs, N.J.: Prentice-Hall, 1954.

360. Veingerov, M. L. A method for gas analysis based on the Tyndall-Röntgen optical-acoustical phenomenon. *Compt Rend Acad Sci* 19:687 (1938).

361. Veingerov, M. L. Spectrophone--an instrument for investigation of infrared absorption spectra of gases and for quantitative and qualitative spectrum analysis of multicomponent gas mixtures. *Compt Rend Acad Sci* 46:182 (1945).

362. Veingerov, M. L. Spectrophone--an instrument for investigation of infrared absorption spectra of gases and for quantitative and qualitative spectrum analysis of multicomponent gas mixtures. *Doklady Akad Nauk* 46:200 (1945).

363. Vidrine, D. W. Photoacoustic Fourier transform infrared spectroscopy of solid samples. *Appl Spectroscopy* 34:314 (1980).

364. Wainstein, L. A., and V. D. Zubakov. Extraction of signals from noise. Englewood-Cliffs, N.J.: Prentice-Hall, 1962.

365. Wake, D. R., and N. M. Amer. The dependence of an acoustically nonresonant optoacoustic signal on pressure and buffer gases. *Appl Phys Lett* 34:379 (1979).

366. Wakefield, T. D. A laser optoacoustic spectrometer for gas concentration measurements. *Proceedings of the Pittsburgh Conference on Analytical Instrumentation*, Cleveland, Ohio, 6 March 1979.

367. Wakefield, T. D., and R. E. Blank. A toxic gas monitor with ppb sensitivity using an automated laser optoacoustic spectrometer. *Proceedings of the Pittsburgh Conference on Analytical Instrumentation*, Pittsburgh, Pa., 3 Mar 1978.

368. Walther, H. Laser spectroscopy of atoms and molecules. Berlin: Springer-Verlag, 1976.

369. Walzer, K., M. Tacke, and G. Busse. Optoacoustic spectra of some far infrared laser active elements. *Infrared Physics* 19:175 (1979).

370. Wang, T. T., J. M. McDavid, and S. S. Yee. Photoacoustic detection of localized absorption regions. *Appl Opt* 18:2354 (1979).

371. Weagant, R. A., and C. H. Beebe. Laser optoacoustic explosives detection. NTIS PB285556, 1977.

372. Wetzel, G. C., and F. A. McDonald. Photoacoustic determination of absolute optical absorption coefficient. *Appl Phys Lett* 30:252 (1977).

373. White, K. O., W. R. Watkins, C. W. Bruce, R. E. Meredith, and F. G. Smith. Water vapor continuum absorption in the 3.5 - 4.0 micron region. *Appl Opt* 17:2711 (1968).

374. Wickramasinghe, H. K., R. C. Bray, V. Jipson, C. F. Quate, and J. R. Salcedo. Photoacoustics on a microscopic scale. *Appl Phys Lett* 33:923 (1978).

375. Wilks infrared spectroscopy accessories. Product bulletin. Analabs Incorporated, North Haven, Conn., 1979.

376. Williams, J. T., and R. N. Hager. The derivative spectrometer. *Appl Opt* 9:1597 (1970).

377. Wintle, H. J. Introduction to electrets. *J Acous Soc Am* 53:1578 (1973).

378. Wong, Y. H., R. L. Thomas, and G. F. Hawkins. Surface and subsurface structure of solids by laser photoacoustic spectroscopy. *Appl Phys Lett* 32:538 (1978).

379. Woodmansee, W. E., and J. C. Decius. Vibrational relaxation in carbon monoxide by the spectophone frequency response method. *J Chem Phys* 36:1831 (1972).

380. Wynne, J. J., and P. P. Sorokin. Optically pumped stimulated emission and stimulated electronic Raman scattering from K atoms. *J Phys B* 8:L37 (1975).

381. Wynne, J. J., P. P. Sorokin, and J. R. Lankard. Laser spectroscopy. New York: Plenum Press, 1974.

382. Yamada, C., T. Aoki, and J. Katayama. Soundwaves excited by a CO<sub>2</sub> Q-switched laser. *J Appl Phys* 40:5404 (1969).

383. Yasa, Z., N. M. Amer, H. Rosen, A. D. Hansen, and T. Novakov. Photoacoustic investigation of urban aerosol particles. *Appl Opt* 18:2528 (1979).

384. Yen, W. M. Photoacoustic and photothermal spectroscopy of ions in solids. NTIS AD66063, 1978.

385. Young, P. H. To detect signals buried in noise, build a phase-locked receiver. *Electronic Design* 12:64 (1971).

386. Zaalberg van Zelst, J. J. Circuit for condenser microphones with low noise level. *Phillips Tech Rev* 9:357 (1947).

387. Zare, R. N. Laser spectroscopy. Proc Second Internat. Laser Spectroscopy Conf., Megeve, 23-27 June 1975. Berlin: Springer-Verlag.

ND  
DATE